UNIVERSITY OF CALIFORNIA
SANTA CRUZ

INFLUENCE OF SOIL CARBON AMENDMENTS ON DENITRIFICATION IN LINKED FIELD AND LABORATORY STUDIES OF MANAGED AQUIFER RECHARGE

A thesis submitted in partial satisfaction
of the requirements for the degree of

MASTER OF SCIENCE

in

EARTH SCIENCES

by

Emily Jane Kam

September 2023

The Thesis of Emily Kam is approved:

_____
Professor Andrew Fisher, chair

_____
Professor Matthew McCarthy

_____
Research Professor Adina Paytan

_____
Professor Samantha Ying

_____
Peter Biehl
Vice Provost and Dean of Graduate Studies

Table of Contents

List of Figures and Table

Figures

Tables

Abstract

Influence of soil carbon amendments on denitrification in linked field and laboratory studies of managed aquifer recharge

by

Emily Kam

This is a study the influence of soil carbon amendments, as part of linked laboratory experiments and field operations, for the cycling of nitrogen compounds during managed aquifer recharge (MAR). The MAR field site is in Watsonville, CA, and collects and infiltrates stormwater runoff on a working ranch. Various soil carbon amendments were applied as permeable reactive barriers (PRBs), including wood chips and almond shells, two carbon sources previously known to enhance microbially mediated denitrification. Intact soil cores were recovered from an infiltration basin and used in flow-through experiments to replicate and extend field observations to quantify substrate controls on biogeochemical processes. For laboratory experiments, PRBs included mixtures of carbon sources and native soil at specific ratios (wood chips 1:1; almond shells 1:1, 1:3, and 1:10). Almond shells mixed with soil as 50% and 25% by volume removed the most nitrate in the laboratory experiments. These two treatments also produced higher amounts of manganese and iron. Elevated levels of these trace metals are interpreted as an indication of a more reducing condition where denitrification can occur more favorably. Wood chips removed a modest amount of nitrate, but also produced nitrite, indicating incomplete denitrification. In field operations, wood chips removed more

nitrate than almond shells but also produced more nitrite. Based on isotopic results, nitrite oxidation may be occurring in the wood chip treated areas. We conclude that, overall, almond shells, at a high enough amount, are a better soil amendment than wood chips for removing nitrate during infiltration for MAR.

Acknowledgements

Thank you to my advisor, Dr. Andy Fisher, for everything: his kindness, understanding, patience, mentorship, and scientific guidance. I will forever be grateful for his help through this winding, mysterious, sometimes terrifying, but ultimately rewarding process. My abilities as a scientist have changed so dramatically the last three years and most of the credit goes to Andy and his incredible ability to push you when you think you can't and make you believe that you are smart enough to accomplish anything. It has been my honor to be his student and learn from his unending spring of knowledge that never runs dry. Thank you, Andy.

I want to thank my committee (Adina Paytan, Matthew McCarthy, and Samantha Ying) for working with tight deadlines and rough, rough drafts. Their invaluable feedback added valuable insights into this work.

Thank you to Kelly Thompson Ranch for allowing us to study on this land. Field days were always special to me, and I was grateful anytime I could go out to sample, install instruments, or recover gear.

This project wouldn't be what it is today with the help of the incredible Hydrogeology group past and present. Adam Price, Jenny Pensky, Kristin Dickerson, Jake Tidwell, and Araceli Serrano – I have learned so much through navigating graduate school by your sides. Thank you for all your support, open ears, and kind hearts.

Thank you to all the incredible undergraduates I have had the absolutely pleasure of working with: Leslie Serafin, Raymond Hess, Eileen Hails, Chloe

Tinglof, Siena Oswald, Manny Rojas, Alex Davani, Emma Schibuola, and Luke Mello. You've worked long and hard hours in the lab and on countless instruments in the MAL. You've acid washed thousands of bottles, made so many Seal reagents, and have always been there when I needed you. Every single one of you is an incredible scientist, and I have learned so much for each one of you throughout this journey. And thank you to Victor Bautista for all your help in the lab and the field. Your incredible talents for hydrogeology helped me build my project from the ground up, and I will always be grateful for your guidance and friendship.

Thank you to my many friends at UCSC that have made my time here so wonderful. I cherish each moment I've spent outside of the lab enjoying my free time and building last friendships.

And finally, thank you to my family for all your love and support through graduate school. Thank you to my dad for his overflowing kindness and generosity. Thank you to Dexter for your distractions while I was trying to write. And thank you to Grant for your love. You have helped me more than you can ever know, and I wouldn't be here today accomplishing this if not for you.

Thank you to the sponsors of this work: the Gordon and Betty Moore Foundation (Award #9964), the USDA/NIFA (Award #2021-67, 019-33,595), USDA/NRCS Resource Conservation Partnership Program (Award #2019-CSA-03), US EPA (Award #RD-84086301-0), and The Recharge Initiative.

Introduction

1.1 Groundwater shortages and water quality issues

Water scarcity is a critical, global problem with high spatial and temporal variability. Groundwater is the world's largest freshwater reservoir (Taylor et al. 2012). In California, groundwater provides 40% of the state's annual water supply during normal years, and a greater fraction in dry years (Babbitt et al. 2018). However, groundwater resources are threatened by excessive extraction, leading to land subsidence, loss of storage, and sea water intrusion into coastal aquifers (Befus et al. 2020). Decreasing water supply is exacerbated by contamination (both point source and distributed) including industrial pollution, leaks from underground tanks, and agricultural activity, naturally occurring metals, and runoff. Nitrate is a common and pernicious groundwater contaminant and is especially difficult to remove once it enters an aquifer. The U.S. Environmental Protection Agency (EPA) found that over 31 million Americans are receiving drinking water with nitrate contamination greater than the maximum contaminant levels set by the Safe Drinking Water Act (10 mg/L), with California being the top affected state (Ward et al. 2006). When drinking water that exceeds the maximum contaminant level is consumed, it can cause methemoglobinemia, or "blue baby" disease in infants (McCasland et al., Shuval et al.)

1.2 Managed recharge and permeable reactive barriers

Managed aquifer recharge (MAR) includes a diverse set of tools and techniques that direct excess surface water into aquifers for the benefit of human and aquatic

systems (Bouwer 2002). MAR can help to balance extractions by enhancing inflows, reducing overdraft, and limiting or reversing seawater intrusion (Masciopinto 2013), loss of baseflow to streams, and degraded groundwater quality (Bekele et al. 2011). MAR has the potential to improve water quality through dilution and enhanced processing of contaminants during infiltration. MAR systems can also function as quasi-natural laboratories for the development of a process-based understanding of carbon, nutrient, and contaminant cycling during soil, water, and microbiological interactions that occur more broadly across landscapes.

The use of a carbon-rich amendment during MAR, applied as part of a permeable reactive barrier (PRB), may improve water quality by inducing heterotrophic denitrification and related processes (e.g., anammox, dissimilatory nitrate reduction to ammonium, and others). Of denitrification, anammox, and dissimilatory nitrate reduction to ammonium (DNRA), denitrification serves as a nitrate sink for aquatic systems (with NO_3 transformed to N_2 gas), whereas anammox and DNRA temporarily immobilize N but do not remove nitrogen as a gas (Korom 1992). Bioavailable soil carbon can stimulate biogeochemical reactions in the shallow subsurface, including enhanced microbial activity (Soares 2000). The denitrification pathway can include a series of intermediate products:

$$NO_3^- \rightarrow NO_2^- \rightarrow N_2O \rightarrow N_2 \quad (1)$$

and can be represented as a redox reaction requiring an electron donor (i.e. carbon):

$$2NO_3^- + 10e^- + 12H^+ \rightarrow N^2 + 6H_20 \quad (2)$$

Denitrification in soils is commonly facilitated by microbial communities that use nitrate as a terminal electron acceptor (Knowles 1982). During sustained saturated conditions, soil pores may become anoxic once available dissolved oxygen is consumed, promoting favorable conditions for denitrification.

Previous studies have shown that a carbon-rich PRB can help to stimulate consumption of oxygen and release of labile carbon, thereby promoting denitrification in shallow soils (e.g., Schipper et al., 2001; Beganskas et al. 2018, Robertson et al., 2000,; Grau-Martínez et al., 2018; Gilbert et al. 2008). Common materials used as carbon sources include wood chips and wood mulch, biochar, and other readily available materials, often associated with agricultural or logging activity. These materials are incorporated into the upper layer of the soil, creating a mixture of native soil and an additional carbon source that functions as a PRB. Earlier studies have also shown that longer retention times (lower flow rates) tend to result in more complete nitrate removal during infiltration for MAR, but PRB materials have an especially strong control on soil redox conditions and the efficiency of denitrification (e.g., Schmidt et al., 2011; Beganskas et al., 2018; Gorski et al., 2019; Pensky et al., 2023).

1.3 Study design and goals

The primary goal of this study is to assess the effectiveness of several PRB carbon amendments that have been applied during infiltration for MAR at an active field site, linking laboratory experiments with samples and data collected in the field. Laboratory experiments were conducted using intact soil cores, recovered from the

base of an active infiltration basin, with flow rates and PRBs that mimic field conditions during MAR operations. The PRB layer used in the field is represented in lab experiments with a "PRB capsule" in terms of composition (native soil ± carbon source) and thickness (~ 30 cm) (Figure 1). This study builds from the results of earlier work and is focused specifically on a setting where the native soil tends to be coarse grained (sandy) and carbon poor.

The focus of this study is Kelly Thompson Ranch (KTR) near the town of Watsonville, central coastal California, in the Pajaro Valley (Figure 2). The Pajaro Valley is located adjacent to Monterey Bay and within the drainage basin of the lower Pajaro River watershed (Figure 2). In the Pajaro Valley over 90% of agricultural and municipal water demands are met with groundwater resources, and there is no imported water, no major rivers or dams, and no annual snowpack. Excessive pumping of regional aquifers has contributed to chronic overdraft, leading to seawater intrusion where aquifer units outcrop against Monterey Bay (Hanson 2003). Land use/land cover in this area is mainly agricultural (~15,000 ha), urban and residential (~7,000 ha), and mixed native and non-native vegetation (39,000 ha) (Beganskas et al., 2019). The main crops include berries, vegetable row crops, grapes, apples, and cut flowers (Garza-Diaz et al. 2019).

The KTR site was constructed in Fall 2019, at the start of the 2020 water year (WY20, 10/1/19 to 9/30/20), including a sediment detention basin with an area of ~1 ac (~0.4 ha) and a primary infiltration basin with an area of ~4 ac (~1.6 ha). The basins are supplied by runoff from around 1,300 ac (~520 ha) of mixed cultivated

areas and rangeland. Dominant surface soils at the field site are Conejo loam, Conejo clay loam, San Emigdio variant sandy loam, and Clear Lake clay (Soil Survey Staff, 2014). The coarser units at KTR appear to comprise the remnants of a paleochannel of a former tributary to the Pajaro River, which runs adjacent to the KTR site at its southwestern end. In general, the soils and shallow underlying units at this site comprise alluvial, fluvial, and floodplain deposits.

The site was selected for a MAR project because the coarse paleochannel deposits comprise a pathway for water to enter underlying aquifers, bypassing finer grained units that are more common at the land surface in the surrounding area. After the infiltration basin was initially constructed, prior to the start of the WY20 wet season, parts of the deepest section of the basin received carbon amendments to form PRB layers, including biochar, aged wood mulch, alfalfa, and almond shells (Table 1, Figure 3). In late 2021, near the start of WY22, soils in part of the basin were amended with conifer wood chips, and an additional plot received a mixture of almond shells and rice husks. In this study, I focus on changes to water quality during infiltration for MAR during WY22 and WY23 and compare these observations to results of flow-through laboratory experiments using soil cores to mimic field conditions.

2. Methods & Materials

2.1 Field site configuration and sampling

2.1.1 Infiltration basin operations and soil amendment

Before the start of each new water year, after the infiltration basin dried, it was scraped to remove accumulated sediment that was deposited the previous water year and disked to open up soil pores. A variety of carbon-rich soil amendments were installed when the basin was initially constructed before the rainy season in WY20. The carbon-rich soil amendments were tilled into the soil with an approximate 1:1 mixture of soil:amendment, creating carbon-rich PRB layers to a depth of 30-40 cm below ground surface (bgs) (Figure 3). A ~2 m^2 area near the northwest side of the basin was augmented with a mixture of almond shells and soil, added by hand with shovels. Mixing and disking was intended to place carbon-rich materials in close contact with native soils and microbial communities, promoting interaction with bioavailable carbon that leaches from the PRB layer, and simplifying subsequent maintenance as part of regular MAR operations. At the start of WY22, conifer wood chips were deposited across the southern ~40% of the infiltration basin and disked to 30-40 cm-bgs, and almond shells and rice husks were added to another ~2 m^2 plot (Figure 3, Table 1). The remainder of the basin was unamended native soil, but uncontrolled mixing of water, sediment, and PRB treatment materials during MAR operations dispersed carbon amendments throughout the basin resulting in no strict "control" treatment in the basin.

2.1.2 Soil sampling

Six intact soil cores, one meter in length, were collected from KTR at Site 03B (Figure 3), in an area that was intended to serve as an untreated control during WY20-23. Cores were collected in Fall 2021, prior to the start of the WY22 rainy season, and after the basin had been scraped following WY21 operations. The cores were collected in adjacent locations, separated by ~30 cm, and additional samples were augered by hand (using a 3-cm diameter bucket) to provide equivalent materials for analyses of sediment texture, composition, organic carbon, nitrogen, and microbiology. These samples will be referred to as "pre-infiltration" when discussing soil solid analyses. The soil cores were collected with a custom coring system comprising a core cutting shoe attached to a 1 m polyvinyl chloride (PVC) tube (10 cm inner diameter, ID), which was manually inserted into the ground with a fence-post hammer (Gorski et al., 2020). The cores were extracted using truck jacks and a pipe dog, then sealed in the field with PVC endcaps for transport back to the lab. Augered soils were sampled at 10-cm intervals to the same depth as the cores (1 m-bgs), from the surface to 100 cm cm-bgs, after placing augered materials on a sediment description and collection board and visually inspecting to assure that both representative and unusual horizons were represented. The samples were bagged individually (plastic for grain size and chemical analyses, and Whirl-Paks for microbiological studies) and returned to the lab for analysis.

2.1.3 Field fluid sampling

Fluid piezometers were installed by hand at seven locations in WY22 and four locations in WY23 (Table 1), to collect pore water samples during infiltration when the basin was operating. Holes were cut with a hand-auger, and piezometers were installed with short screens centered at 30 cm-bgs and 50 cm-bgs, and a subset of piezometer locations were instrumented with bottom-water intakes using a similar design. Piezometers were constructed from acrylic tubes wrapped in nylon mesh and surrounded in the soil with rounded, well sorted, 1-2 mm quartz sand. The individual sampling depths at a single location were separated and sealed by 5-8 cm of bentonite clay, and holes were backfilled with native soil. Nylon tubes were run from the piezometers up the side of the infiltration basin to sampling posts, and tubing was capped to limit contamination between sampling rounds. During rain events when there was standing water in the infiltration basin, a peristaltic pump was used to collect water from the piezometers, and samples were collected into 125 mL HDPE bottles and glass vials with crimp caps for dissolved inorganic carbon. A nearby shallow farm well (screen depth ~25-40 m bgs) was sampled during infiltration sampling and at additional (generally quarterly) intervals.

2.2 Laboratory operations and sampling

Upon return from the field, core ends were opened, coarse (1-2 mm diameter) silica sand and glass wool was inserted, and cores were re-capped and stored at 15 °C until testing could begin. Tests were run as two sets of three cores, with each set of tests run concurrently with a single peristaltic pump and drive head and three separate

fluid lines fed by a single tank of synthetic stormwater. During testing, each core was placed in sequence with a 30 cm section of the same PVC tube used for coring (ID = 10 cm), filled with either shallow native soil from the infiltration basin (as a control) or a mixture of this soil and a carbon-rich amendment (Figure 1, Table 2). These short sections of PVC containing PRB, and native soils are referred to herein as "PRB capsules." The soil cores were inverted for flow experiments such that the top of the soil core (the surface in the field) was at the bottom in the lab, immediately following the PRB capsule in terms of fluid flow (Figure 2). Inversion of the soil core allowed pumping of fluid up through the core, preventing drainage and ensuring continuous saturation. The experiment was intended to test a range of flow rates, but due to difficulty in maintaining consistent flow rates with the pump system, flow rates are not analyzed as an independent variable. Earlier work suggests that the PRB amendment is one of the most important parameters in determining biogeochemical response to infiltrating fluids (Pensky et al., 2023), so the focus in this study is on PRB treatment. To reduce flow-rate dependence, all data shown from laboratory experiments in this study are from measured flow rates of ≤0.6 m/day, a range that allows for considerable biogeochemical processing (e.g., Schmidt et al., 2011; Gorski et al., 2019).

Synthetic storm water used in this study was supplied with a 500 L tank filled with local tap water mixed with dissolved potassium nitrate ($K\text{-}NO_3$), as a proxy for nitrate-rich runoff. Influent nitrate concentrations ($[N\text{-}NO_3]$) during the experiments discussed in this study ranged from 5.3 to 14.0 mg/L. Although lower concentrations

of nitrate are typically found in the field at KTR, higher concentrations were tested to assess limits for the denitrifying capabilities of the PRB materials. Both the PRB capsules and soil cores were instrumented with Rhizon pore fluid samplers with a pore size of 0.6 μm along a 5 cm glass fiber sampling membrane rod. Samplers were installed at 20 cm intervals along the soil cores; this study reports results only from influent, outflow from the PRB capsules, and pore fluids extracted using the final sampler at core outflow (Figure 2).

The first set of experiments ran for 95 days with 55 days of sampling, and the second set of experiments ran for 110 days with 39 days of sampling. During sampling, a sterile, acid washed Luer lock 60 mL syringe was attached to a Rhizon pore fluid sampler and was pulled open to create suction, then held with wooden blocks to allow the syringe to fill. Sampled fluid was passed through a 0.2 μm syringe filter and into acid-washed and labeled high density polyethylene (HDPE) bottles, then frozen at 15 °C until analyses were completed. After each set of infiltration experiments, soil cores were split longitudinally on the benchtop and soil was sampled at 10-centimeter intervals, corresponding to the samples collected directly in the field by hand auger. These post-experiment samples were analyzed for texture and chemical composition to assess differences associated with the flow experiments and PRB treatments. For this comparison, materials collected by auger are considered to represent "pre-infiltration" conditions, whereas materials collected from the cores after the infiltration experiments are referred to as "post-infiltration" samples.

2.3 Analytical analysis

2.3.1 Solid samples

Soil samples collected for soil textural analysis were stored in plastic bags until processed for analysis. For each sample, a subsample (5-6 g) was placed in a 125 mL LDPE bottle and treated with 20-50 mL of a 30% H_2O_2 solution, which oxidizes organic matter and decomposes it into carbon dioxide and water (Mikutta et al., 2005), then freeze dried to create a soft powder. Grain size distributions were measured using a liquid suspension of treated sediment, with a sodium hexametaphosphate deflocculant, in a Beckman Coulter LS-13320 Particle Size Analyzer (PSA), which uses laser diffraction spectroscopy to determine the distribution of particle diameters (Beckman Coulter, 2011). Soils were classified in terms of fractions comprising sand, silt, and clay (63 µm to 2 mm, 4 to 63 µm, and <4 µm, respectively).

Soil samples collected for carbon and nitrogen analyses (concentrations and $\delta^{15}N$ and $\delta^{13}C$ isotopes) were homogenized with a mortar and pestle and freeze-dried. Samples were analyzed on a CE Instruments NC2500 elemental analyzer coupled to a Thermo Scientific DELTAplus XP isotope ratio mass spectrometer (EA).

2.3.2 Fluid samples

Fluid samples (both field and laboratory) were measured for dissolved organic carbon (DOC), dissolved inorganic carbon (DIC), nutrients (nitrate and nitrite), metals (Fe, Mn, As), and isotopes of nitrate ($\delta^{15}N$ and $\delta^{18}O$). All fluid samples, except for those analyzed for DIC, were filtered at 0.2 µm. DOC samples were stored in 15

mL glass vials with silicone septa, then analyzed using a Shimadzu TOC-VCPH analyzer. DIC samples were collected in 15 mL glass vials with crimp caps, then analyzed on a UIC Carbon Coulometer. Nutrient samples were collected in 15 mL plastic Falcon tubes and analyzed on a Lachat QuikChem 8000 Flow Injection Analyzer and/or a SEAL Segmented Flow Analyzer AA500. Nitrogen isotopes were collected in 20 mL HDPE bottles and sent to the Stable Isotope Facility at UC Davis for analysis.

For field samples three samples were analyzed per treatment: influent, 30 cm-bgs, and 50 cm-bgs. For lab samples, three samples per treatment were analyzed: influent, PRB capsule, and effluent (100 cm). Samples with [N-NO2] were treated with sulfamic acid to remove all nitrite. Results for changes in both [DOC] and [N-NO3] will be presented in this study. We define a delta value (e.g., △[DOC] and △[N-NO3]) as a deeper sample's concentration subtracted from a shallower sample's concentration, leading to values < 0 when the analyte was consumed, and values > 0 when the analyte was produced.

3. Experimental Results

3.1 Chemical and physical soil characterization

3.1.1 Soil texture

Soil textures are consistent across post-infiltration and pre-infiltration samples used in this study, as expected. The median grain size in all cores is 256 (±21.1) to 277 (± 42.9) μm (medium-grained sand) (Table 3). The distributions of all samples are unimodal and left-skewed with little variation between soil cores (Figure 4).

There are subtle textural variations with depth along the six soil cores tested, and the primary textural assignments are: 82.7 – 97.7 % sand, 1.7 – 12.7 % silt, and 0.6 – 6.7 % clay.

3.1.2 Soil C and N content

In the pre-infiltration samples, the median carbon content across all depths is 2400 ± 300 (ppm). The two post-infiltration cores analyzed, NS and ALM50, have median soil carbon contents of 2250 ± 370 ppm and 2050 ± 520 ppm respectively (Table 4). Within the variation, none of the medians are significantly different from one another. There are also no clear trends with depth in pre- and post-infiltration samples, although we observe one sample with elevated [C] in the native soil (NS) treatment at 40 cm-bgs. (Figure 5A).

Median [N] in soils from pre-infiltration is 125 ± 15 ppm, with higher values near the ground surface (Figure 5). Post-infiltration [N] concentrations are essentially identical to each other, 170 ± 30 ppm (NS treatment) and 175 ± 22 ppm (ALM50 treatment). Median [N] in the post-infiltration cores are higher than observed in the pre-treatment samples. All three sets of samples have decreasing [N] with depth below ground, from 0 to 100 cm-bgs, and the two post-infiltration cores show larger variability in [N] with depth compared to the pre-infiltration samples.

$\delta^{13}C$ values from both post- and pre-infiltration samples have similar values and trends with depth (Figure 6A). The median values for pre-infiltration and post-infiltration (NS and ALM50) are -12.7 ± 3.4 ‰, -11.8 ± 2.2 ‰, and -11.4 ± 1.6 ‰ respectively. The median values for AUG, NS, and ALM50 are -0.5 ± 0.8 ‰, -3.2 ±

2.5 ‰, and -4.0 ± 1.9 ‰. The pre-infiltration samples have isotopic values that are consistently heavier than the post-infiltration samples through the depth range sampled.

3.2 Fluid chemistry results

3.2.1 Dissolved organic carbon and dissolved inorganic carbon

[DOC] in pore fluids recovered from sediments of the operating MAR system do not show significant differences between treatments, but there are small differences with depth in each treatment (Figure 7). NS samples show a slight trend of increasing [DOC] with depth, from ~8 to 13 mg/L, whereas the WC treatment shows consistent values with depth of ~10 mg/L, and the ALM treatment shows higher values in influent (~20 mg/L) and lower values with depth, ~12 mg/L and 17 mg/L at 30 and 50 cm-bgs, respectively.

[DOC] in pore fluids from lab experiments also do not vary significantly between treatments (Figure 8). The majority of the cores also do not vary much with depth, with the exception of ALM25, which have some higher [DOC] values at 60 cm.

There are differences between Δ[DOC] measured in the PRB capsules ($\Delta[DOC]_{PRB}$), soil core ($\Delta[DOC]_{SOIL}$), and overall system ($\Delta[DOC]_{TOTAL}$) (Figure 9). None of the Δ[DOC] values vary significantly among treatments, based on p-values from Pairwise Willcox tests (Tables 5-7). Observing patterns in individual cores, ALM10, ALM25 and WC have higher magnitude $\Delta[DOC]_{PRB}$ then $\Delta[DOC]_{SOIL}$. ALM25 and ALM10 both have positive median $\Delta[DOC]_{SOIL}$ values, meaning there

was an apparent increase in carbon in pore fluids during flow through the soil column (Figure 9).

The median of dissolved inorganic carbon ([DIC]) concentrations in pore fluids collected in the field are ordered as: $[DIC]_{WC} > [DIC]_{NS} > [DIC]_{ALM}$ (Figure 10). However, there is enough variability and overlap between the field [DIC] values that treatment results are not statistically different (Kruskal-Wallis test, $p = 0.207$). The core [DIC] values also vary by treatment with significant differences. NS has the lowest median [DIC] values and ALM50 has the highest. ALM50 and WC have significantly higher [DIC] than NS (Pairwise Willcox test, $p = 0.033$ and $p = 0.00048$ respectively, Figure 11, Table 8).

3.2.2 Nitrogen species (nitrate, nitrite, and ammonium)

In KTR field samples, there is no nitrate removed with depth in the sampling locations that have native soil or almond shell PRB layers (Figure 12). In contrast, the samples from the locations with a wood chip PRB layer show significant [$N\text{-}NO_3$] differences with depth, especially between 30 cm-bgs and 50 cm-bgs. All surface and shallow subsurface samples show significantly less nitrate than concentrations seen in the shallow farm well (Figure 13). The well has an average [$N\text{-}NO_3$] of 17.8 ± 5.3 mg/L whereas all field samples have an average [$N\text{-}NO_3$] of 0.95 ± 0.61 mg/L. Comparing Δ[$N\text{-}NO_3$] of all three treatments based on field data, wood chips clearly removed more nitrate than either native soil or almond shells (Figure 14).

Nitrate concentration trends in laboratory experiments (Figure 15) show similarities in the NS and WC treatments to the field data. There is no change in [N-

NO_3] with depth in the NS core, but a significant decrease in [N-NO_3] from the influent to the PRB capsule of the WC treatment. ALM25 show similar patterns to WC except with lower overall median nitrate values throughout the soil core. The ALM50 treatment shows a gradual reduction in [N-NO3] from influent to PRB to the first soil sample. ALM10 also shows a greater [N-NO_3] decrease from the influent to the PRB sample, compared to ALM50, but also has higher median nitrate concentrations in pore fluids from the soil core compared to both ALM50 and ALM25 treatments.

As was calculated for [DOC], Δ[N-NO_3] was analyzed for the PRB capsules ($\Delta[N\text{-}NO3]_{PRB}$), soil cores ($\Delta[N\text{-}NO3]_{SOIL}$), and overall systems ($\Delta[N\text{-}NO3]_{TOTAL}$) used for laboratory experiments. In the PRB capsule, both ALM50 and ALM25 are significantly different from NS (Pairwise Willcox test, $p = 0.0079$ and $p = 0.024$ respectively, Table 9, Figure 16). However, within the PRB, all cores show nitrate removed (median $\Delta[N\text{-}NO3]_{PRB} < 0$). In the soil core, once again ALM50 and ALM25 removed significantly more nitrate than did the NS treatment (Pairwise Willcox test, $p = 0.068$ and $p = 0.012$ respectively, Table 10, Figure 17). Both the NS and WC median $\Delta[N\text{-}NO3]_{SOIL}$ values are positive (indicating addition), whereas the three almond shell treated cores have negative $\Delta[N\text{-}NO3]_{SOIL}$ (indicating removal). In the total system, ALM50 and ALM10 vary significantly from each other, with ALM50 removing more N-NO_3 than ALM10 (Pairwise Willcox test, $p = 0.070$, Table 11, Figure 18). ALM50 and ALM25 also removed significantly more nitrate than the control native soil core but are not significantly different from each other (Table 11).

Overall, the ALM10 and WC treatments did not remove significantly more NO_3 than did the NS treatment. All of the cores have negative median $\Delta[\text{N-NO3}]_{TOTAL}$ values.

Nitrite ([N-NO_2]) in KTR field samples tend to be low, generally ≤0.05 mg/L, but there are some patterns with depth. Native soil shows a slight decrease in [N-NO_2] with depth, whereas both wood chips and almond shells increase (Figure 19). There are higher and more variable [N-NO_2] values in pore fluids sampled from cores during laboratory experiments (Figure 20). NS has no overall trend with depth, although there are slightly higher values in the PRB capsule. [N-NO_2] in pore fluids from the WC treatment increase significantly from the influent, with median values rising to near 1 mg/L at 100 cm depth. ALM50 have elevated median [N-NO_2] values at 20-60 cm depths, followed by a decrease at 100 cm. Both ALM25 and ALM10 have low median concentrations of nitrite and do not show consistent patterns with depth, although the ALM25 treatment is notable for high temporal variability.

Ammonium ([N-NH4]) in field samples did not vary significantly, but all samples have low concentrations, with most values < 0.1 mg/L (Figure 21). Higher values are seen in laboratory experiments in some core samples. NS and WC show values similar to the field with median [N-NH4] values being ≤ 0.1 mg/L (Figure 22). ALM25 shows the most temporal variability and overall highest median values. ALM10 only has elevated [N-NH4] values in the PRB capsule.

3.2.3. Nitrogen isotopes

KTR field $\delta^{15}N$ values range from 6.87 – 15.00 ‰ and $\delta^{18}O$ range from 5.98 – 10.87 ‰ across all treatments (Table 13, Figure 23). ALM samples show no pattern with depth and very small changes in both $\delta^{15}N$ and $\delta^{18}O$ (ranges of 7.60 – 7.98 ‰ and 6.44 – 6.93 ‰ respectively). NS samples have little change in $\delta^{15}N$ (7.43 – 7.98 ‰) but lighter $\delta^{18}O$ with depth. The WC treatment has the largest change in both $\delta^{18}O$ and $\delta^{15}N$. From influent to 30 cm-bgs, both values decrease, but from 30 cm-bgs to 50 cm-bgs both increases.

Lab samples differ from field samples in several ways. $\delta^{15}N$ values were 0.30 – 12.16 ‰ and $\delta^{18}O$ values were 44.05 – 57.77 ‰ across all treatments (Table 13, Figure 24). ALM50 has a positive slope with increasing depth from influent to effluent ($\delta^{15}N$ changed from 0.36 to 9.16 ‰ and $\delta^{18}O$ from 49.62 to 57.77 ‰). The cross plot for ALM10 also has a positive slope ($\delta^{15}N$ changed from 0.42 to 4.58 ‰ and $\delta^{18}O$ from 51.83 to 53.31 ‰). The WC treatment in lab experiments, unlike the equivalent treatment for field samples, decrease in $\delta^{18}O$ (from 50.71 to 44.05 ‰) and increase in $\delta^{15}N$ (0.30 to 12.16 ‰) resulting in a negative slope on the cross plot (Figure 24). NS show no clear pattern in $\delta^{18}O$ versus $\delta^{15}N$.

3.2.4 Trace metals in fluids

Field arsenic concentrations [As] in pore fluid samples are the highest in the native soil samples and lower in fluids from both the wood chip and almond shell treatments (Figure 25). However, the medians of all treatments and all depths are ~ 4 ug/L. In all treatments there are no clear patterns with depth. Manganese

concentrations [Mn] in pore fluids are highest in the almond shell samples (Figure 26). In all treatments, [Mn] tends to decrease with depth. [Mn] in WC and NS are all < 0.02 mg/L, while ALM reaches a high of ~0.08 mg/L. Iron concentrations [Fe] in pore fluids are higher in the two areas treated with a carbon amended PRB layer than in the native soil. Both wood chip and almond shell treatments result in an increase in [Fe] with depth (Figure 27). All medians are between 50 – 100 ug/L, except for ALM 50 cm-bgs of 385 ug/L.

In laboratory experiments, the ALM25 treatment has the highest concentrations of arsenic in pore fluids in comparison to the other treatments (Figure 28). In all cores except for NS, [As] tend to increase towards the middle of the soil core and then decrease towards the effluent. All cores except for ALM25 have medians of <5 mg/L. In ALM25, except for the PRB, all medians are higher, reaching a maximum median [As] concentration of 21 mg/L. [Mn] is elevated in the ALM25 treatment with increasing values towards the effluent, and the WC treatment show a similar trend with lower magnitude (Figure 29). [Mn] in the NS treatment was consistently low. In all cores except ALM25, all medians are <1 mg/L. The highest median in ALM25 at 60 cm is [Mn] = 2.6 mg/L. [Fe] in pore fluids from laboratory experiments have more variation between different treatments than did [Mn]. [Fe] in ALM25 and ALM50 treatments have significantly more iron in portions of their cores compared to the other treatments and the control (Figure 30). [Fe] in the PRB capsule of the ALM50 treatment is highly elevated (median = 290 ug/L), but [Fe] was much lower in the associated soil core. The ALM25 treatment also has high [Fe] in the PRB capsule

(median = 563 ug/L) and elevated values extending to the shallowest sampling points in the sediment core, at 20 cm (median = 540 ug/L) and 40 cm (median = 178 ug/L), with a return to lower values at greater depth (Figure 29). [Fe] in NS, WC, and ALM50 treatments are modestly elevated, with observed concentrations generally ~5-20 µg/L, with no apparent trends with depth.

4. Discussion: Interpretations and Implications

4.1 The influence of infiltration on soil chemistry

The soils at the field site and used in the laboratory experiments were mostly medium to coarse sand that was very low in carbon and organic material. Similar tests run with samples from other sites often used cores that were finer grained and richer initially in organic carbon (Gorski et al. 2019; 2020; Pensky et al. 2023). The sediments tested in the present study did not vary significantly from one another in terms of soil texture. Sample homogeneity was the desired result of collecting the cores and auger samples in immediately adjacent locations in the KTR infiltration basin. By achieving similar soil texture, we intended to limit the potential influence of differences in grain size between cores and other samples. On this basis, we focus mainly on differences in results due to PRB treatment type.

In the pre-infiltration soil samples, there are slight variations in carbon content (Figure 5A). However, there is no statistically significant changes in carbon content when comparing pre-infiltration to post-infiltration (Kruskal-Wallis test: H=2.36, df=2, p = 0.31). These results suggest that the soil carbon content was not much affected by the added organic carbon associated with an overlying/upstream carbon

rich PRB. This contrasts with an earlier study, using generally finer and more carbon rich material from a flood plain, where there were smaller amounts of carbon in cores treated with a PRB capsule (Kam et al., 2021). Other studies noted that the presence of clay minerals and higher organic carbon concentrations in solids may influence the nature of microbial populations, with greater initial diversity and or abundance of some populations, including denitrifiers (Li et al. 2019). Samples were collected for microbiological analyses associated with the present study, but this work is not yet completed. We suspect that, because the KTR soils tend to be mainly coarse sand, with low soil organic carbon, initial microbial populations may be low, as seen earlier studies of sandy soils (Beganskas et al., 2018; Pensky et al 2023).

4.2 Relationship between denitrification and DOC

Anammox (anaerobic ammonium oxidation), dissimilatory nitrate reduction (DNRA), and denitrification are processes that remove nitrate from the environment; data collected in the present study suggest that denitrification occurred in both the laboratory experiments and field operations. Conditions appear to have been strongly reducing based on the mobilization of arsenic and manganese in the columns that had the added carbon amendment. We know that once the oxygen has been consumed by microbes, the next most energy efficient oxidant. Anammox requires nitrite to oxidize ammonium to nitrogen gas. As mentioned above, in anoxic conditions, nitrate can be reduced by denitrifying bacteria but can also be converted by ammonium during DNRA which releases nitrite as an intermediate product (Kumar et al, 2010). However, we do not see elevated levels of ammonium or nitrite in any core or field

sample. Although this does not exclude the possibility that these intermediate products were produced and then consumed quickly, it seems likely that denitrification occurred during infiltration in the laboratory and field. A study on anammox in a freshwater aquifer found that this process is favored when there is a restricted electron supply (Smith et al., 2015). Our systems were not constrained by an electron supply (given abundant bioavailable carbon in PRB layers), consistent with denitrifying bacteria were using organic carbon to consume nitrate. The conditions in this study were not as compatible with anammox. To be sure, all of these processes (and other processes involved in nitrogen cycling) could have occurred – but there is abundance of evidence consistent with denitrification being an important process that can account for nitrate removal.

Both field and laboratory observations suggest that the nature of a carbon rich PRB treatment influences the extent of denitrification in shallow soils during infiltration (Figures 12, 14, 15-18]. However, the extent of denitrification is not consistently correlated with [DOC] present in pore fluids (Figure 31). There is relatively little difference in [DOC] across the treatments, yet there are a large range of [N-NO3] values. Although there may be subtle patterns based on PRB type, the trends are not significant enough to draw direct correlations between [DOC] and PRB type. However, there were patterns in [N-NO3], where ALM25 and ALM50 tended towards greater nitrate removal. Generally speaking, there is no correlation between amount of Δ[DOC] and Δ[N-NO3]. One possible explanation is that the species of bioavailable organic carbon compounds released from the PRB materials differed

such that some were more readily taken up or energetically more favorable and used by denitrifying microbes. We also note that [DOC] in pore fluids is a measure of the "standing stock" and may therefore not be indicative of how much [DOC] was released by the PRB and subsequently processed quickly by microbes. Another explanation for the lack of variation in [DOC] is that the organic carbon measured in the fluids was mainly refractory and so wouldn't be as readily consumed by microbes. Thus, the concentrations would not change in large amounts. Other elements were also being released throughout the infiltration process and could have affected the extent to which denitrification occurred. For example, higher amounts of iron were found in the two columns that removed the most amount of nitrate (Figures 18 and 30). Studies have shown that iron-dependent denitrification can occur where iron acts as the electron donor (Equation 3) for denitrifying bacteria (Li et al., 2023).

$$\mathrm{Fe(II)} + 2\,\mathrm{NO_3^-} + 12\,\mathrm{H^+} \rightarrow 10\,\mathrm{Fe(III)} + \mathrm{N_2} + 6\,\mathrm{H_2O} \qquad (3)$$

Although there is no clear correlation between amount of [DOC] and denitrification rates, different PRB types and amounts removed different amounts of nitrate. As stated above, in the lab, ALM50 and ALM25 removed the most amount of nitrate (Figure 18). In the field, WC removed the most nitrate (Figure 14). The ALM50 and ALM25 treatments in removed more carbon than did the ALM10 treatment.

4.3 Comparison of PRB treatments

Nitrite is an intermediate product of denitrification. WC in both the field and the lab have elevated levels of nitrite compared to the control and the almond shell treatments. The presence of nitrite could be interpreted as incomplete denitrification (intermediate product not consumed). Based on laboratory experimental data, it appears that the ALM50 and ALM25 treatment are more effective soil treatments because they have more completely removed nitrogen from the system. The ALM10 treatment did not remove as much nitrate, even though that core contained minimal amounts of nitrite and ammonium. The WC treatment also did not remove as much nitrate and produced more nitrite.

Isotopic data from laboratory experiments also suggest that denitrification occurred in the almond shell treatments but not in the wood chips (Figure 24). Both ALM50 and ALM10 treatments have trends similar to a canonical 2:1 denitrification slope (Granger et al., 2008). A negative slope (decrease in $\delta^{18}O$ with an increase in $\delta^{15}N$) could indicate nitrite oxidation (Casciotti 2016), perhaps as a consequence of nitrite being oxidized, although the potential source of oxygen remains enigmatic.

4.4 Trace metal contamination and trends

The ALM25 treatment show elevated levels of As, Fe, and Mn compared to the other treatments applied during core experiments. All three trace metals increase in concentrations near the top or middle of the cores and then decrease towards the effluent. Iron is unique in that the highest levels are found in the PRB capsule and shallow soil. This could imply more reducing conditions in the middle of the core,

with oxidating conditions at the top and bottom. This was surprising, as there should be no source of oxygen that allowed a return to oxidating conditions once reducing conditions were established. There was no evidence for air leakage into the core to cause oxidation and thus adsorption of metals back into the solid phase. Iron levels are two orders of magnitude higher in the PRB capsule of ALM50 and in ALM25. These two cores removed the most nitrate, consistent with a link between these processes. As noted previously, elevated iron levels could have aided in iron-dependent denitrification.

4.5 Comparing to previous work

Work in this study is partially consistence with previous studies that also conducted flow through infiltration columns comparing different PRB materials (Pensky et al., 2023). One of the major findings in that work was that an almond shell PRB removed the most amount of nitrate in comparison to other PRBs and only native soil. This study also found that ALM (at a threshold ratio with native soil) performed better than WC and the control native soil in laboratory experiments. This study differs mainly in the [DOC] and trace metal results. Pensky et al. (2023) saw differences in the amounts of [DOC] being released from the different treatments, with almond shells releasing the most. In contrast, we do not see large differences in the amount of [DOC] released from different treatments in the lab experiments yet noted significant differences in the amount of nitrate removed by each treatment (Figure 31). The trace metal results also differ between the two studies. In general, higher metal concentrations were found by Pensky et al. (2023). Although iron levels

are high in the PRB and shallow soil samples in the ALM50 and ALM25 cores, concentrations in effluent are low for all treatments. In comparison, the ALM effluent in cores tested by Pensky et al. (2023) were consistently high, perhaps because of differences in the native soil compositions.

4.6 Comparing laboratory and field results

Although field data are limited, there were consistent behaviors observed in the laboratory and field. [DOC] in both the field and lab did not vary significantly by treatment or with depth (Figures 7 and 8). The field samples did have, on average, more [DOC] than lab samples (~ 10 mg/L and ~ 4 mg/L respectively). We attribute the higher [DOC] in the field to a greater fraction of PRB material. There was on average more [DIC] in the laboratory samples than the field samples (Figure 10 and 11). Higher [DIC] can be caused by higher rates of respiration by microbes in the soil (carbon dioxide produced). Elevated [DIC] in the lab could be explained by warmer temperatures compared to the field and so would promote more microbial activity and growth.

However, the field almond shell samples have lower [DIC] than the native soil compared to lab results where all three almond shell cores have higher [DIC] than NS. In the field experiment, wood chips outperformed almond shells in terms of nitrate removal (Figure 12). We could not control pore fluid flow rates in the field, and one possibility is that flow rates in the field were greater, limiting pore fluid retention time, a factor that is known to influence denitrification rates (Gorski et al. 2020). [N-NO2] values in pore fluids extracted below the WC treatment in the KTR

basin increased with depth and were much higher than observed in both the native soil and almond shells treatments. This is consistent with the laboratory results showing higher [NO2-N] in pore fluids from core below the WC PRB. The accumulation of nitrite in pore fluids generally indicates a bottleneck in the denitrification process, and/or more rapid generation of [NO2-N] compared to consumption. One possible explanation for both the lab experiment and field treatment with the WC PRB, nitrite consumption could not keep up with the rate of production. In this regard, wood chips may comprise a less effective PRB material for promoting denitrification compared to almond shells.

There are differences in trace metal concentrations between the field and the lab. ALM25 has the anomalously high arsenic concentrations; much higher than the field almond shell samples (Figure 25 and 28). We speculate because only ALM25 have higher concentrations, almond shells are not inherently associated with higher arsenic. Manganese concentrations are consistently higher in the lab than the field (Figures 26 and 29). Higher manganese is associated with more reducing conditions (Davison et al., 1982). The cores were kept saturated during the experiment, whereas field conditions contained periods of wetting and drying. Therefore, we assume that lab conditions were more reducing than the field. Iron in the cores ALM50 and ALM25 are higher than iron concentrations found in the field. These higher concentrations in the lab could also be a result of the more saturated, reducing conditions.

Overall, the laboratory and field samples exhibited some similar chemical behaviors. The most significant difference was that wood chips removed more nitrate than almond shells in the field, whereas we observed the opposite in the laboratory experiments. In the lab, we were able to control the exact amounts of PRB material that was tested in each column. Due to this, we believe that almond shells are the best soil amendment for denitrification. It is also important to reiterate the elevated levels of nitrite in the wood chip samples in both the field and the lab, indicating that this type of PRB resulted in partial denitrification.

5. Conclusions, future work, and implications for MAR

In this study we ran a linked laboratory and field MAR experiment testing different types and amounts of PRB. There are no significant differences in the amount if organic carbon that each PRB treatment gave off in either the field or the lab, yet there were differences in the amount of nitrate removed. Based on the total nitrogen removed from the system, we assert that ALM50 and ALM25 are the best treatments for denitrification. The field results show that wood chips outperform the almond shells in terms of nitrate removed. However, there is significantly more nitrite in wood chips samples leading us to believe that incomplete denitrification may have occurred. Although the lab was not an exact proxy for the field, there were many chemical similarities. Variables including temperature, saturation, and flow rate are all factors that would have created discrepancies between the two experiments. We recommend that field MAR projects use almond shells as soil amendment where accessible. In California where in 2023 it is projected that the state will produce 2.6

billion pounds of almonds (USDA, 2023) using the waste products can be a sustainable way of augmenting MAR projects It should be noted that other products including wood chips are effective promoting microbially mediated denitrification and if those supplies are more readily available can be used. In future work, hydrogen nuclear magnetic resonance (^{1}H NMR) will be done on leachate samples from different PRB materials to help elucidate on a more precise level why wood chips and almonds shells act differently. This has the potential to better constrain the types of organic carbon that are preferentially used by the microbially communities. With growing threats on fresh water supplies, PRB enhanced managed aquifer recharge is an inexpensive and straightforward method to increase available water to both agriculturally and urban communities.

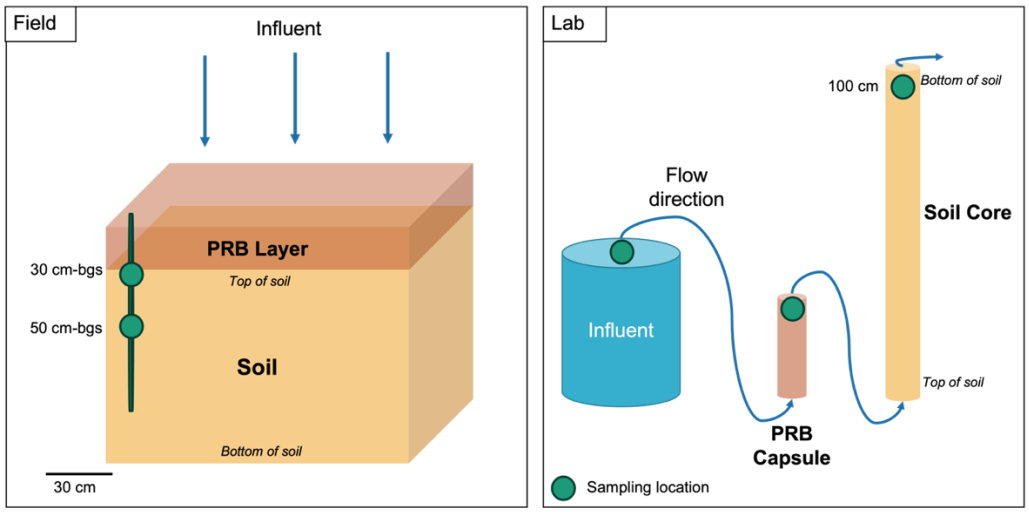

Figure 1. A. Schematic of field depth profile showing PRB layer applied to the top 30 cm of the soil, underlying soil, and piezometer with two subsurface sampling locations at 30 and 50 cm below ground surface. Inflowing stormwater at the field site flows downward through the soil as indicated by arrows. B. Experimental set up in laboratory, with core inverted and flow upwards through the PRB capsule and soil core, using synthetic stormwater. Three sampling locations (of the seven total) are depicted: Influent, PRB capsule, and effluent of the soil core.

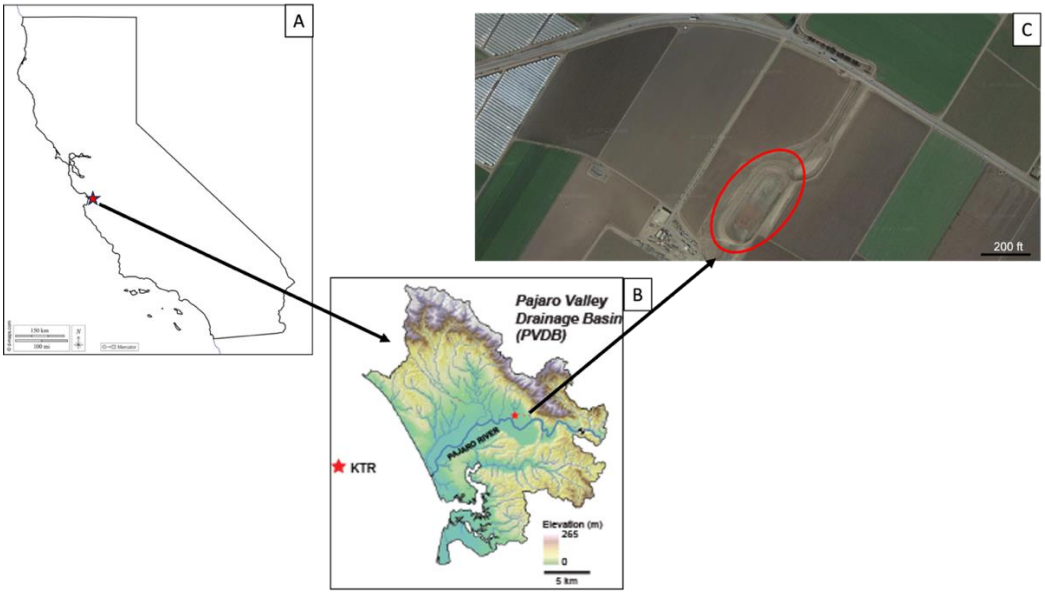

Figure 2. A. Map of California with a star indicting Watsonville, CA the location of the field site. B. Parajo Valley Drainage Basin with a star denoting location of Kelly Thompson Ranch (KTR) infiltration system. C. KTR infiltration basin.

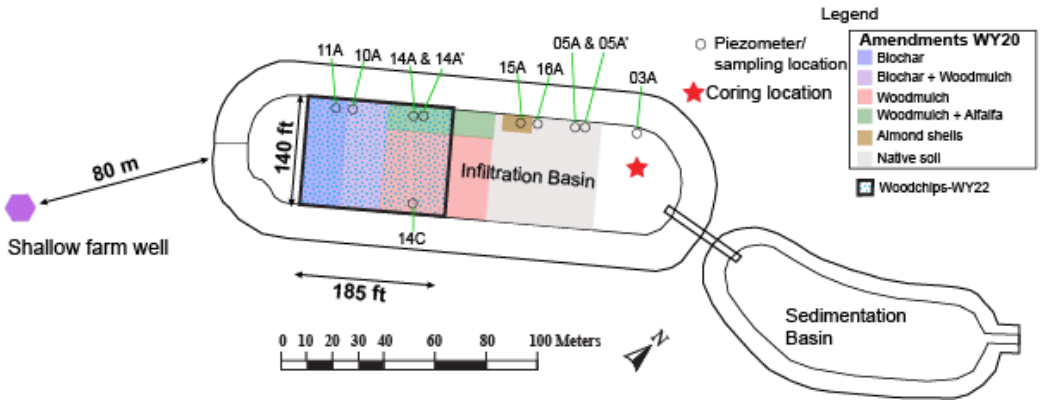

Figure 3. Schematic of KTR infiltration basin and connected sedimentation basin. PRB layers for WY20 and WY22 are marked and defined. Additionally, the location of the coring is marked with a red star and the shallow farm well is in purple.

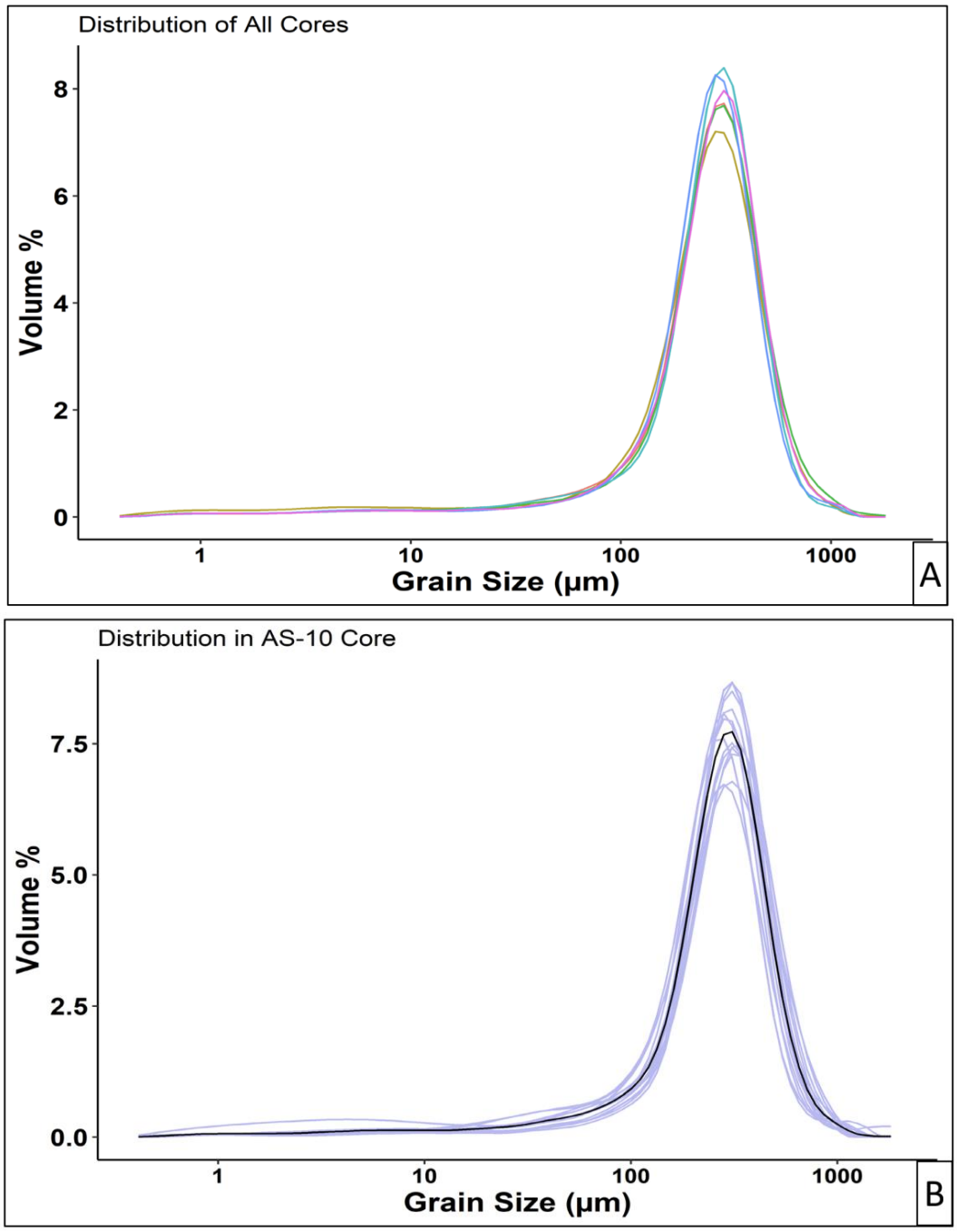

Figure 4. Distribution of grain size by volume percent. (A) Distribution averaged for all samples within each core, with each line representing average of individual cores. (B) Distribution within the ALM10 core, with the black line representing the average of all depths.

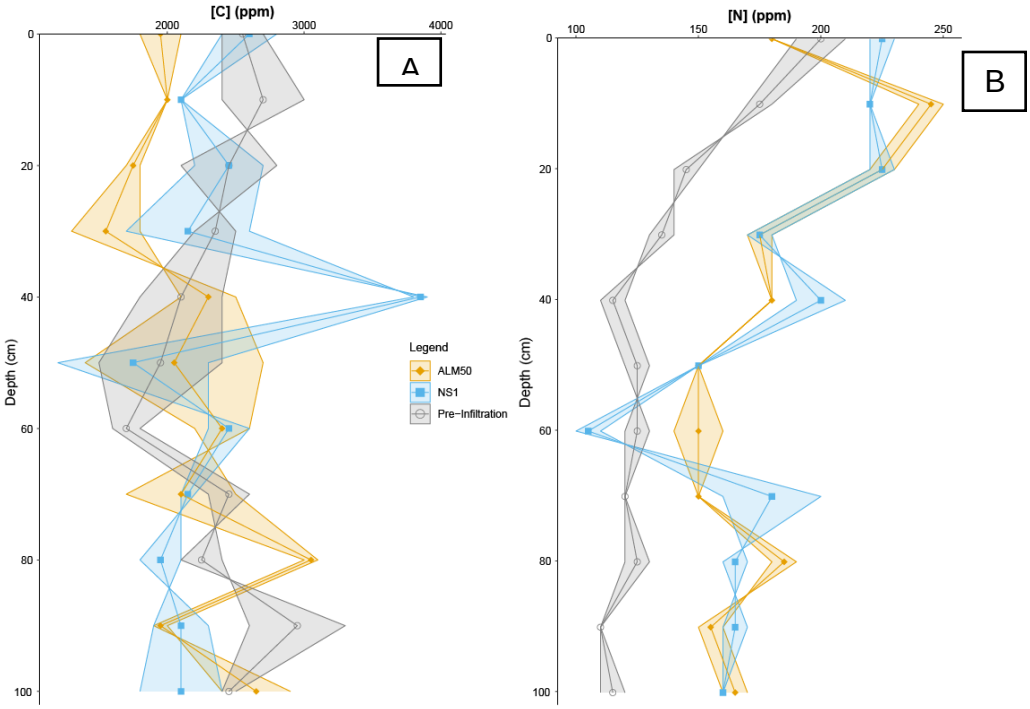

Figure 5. Carbon content (A) and nitrogen content (B) in soil samples showing comparison between cores (native soil and almond shell 50%) and pre-infiltration soil samples in gray.

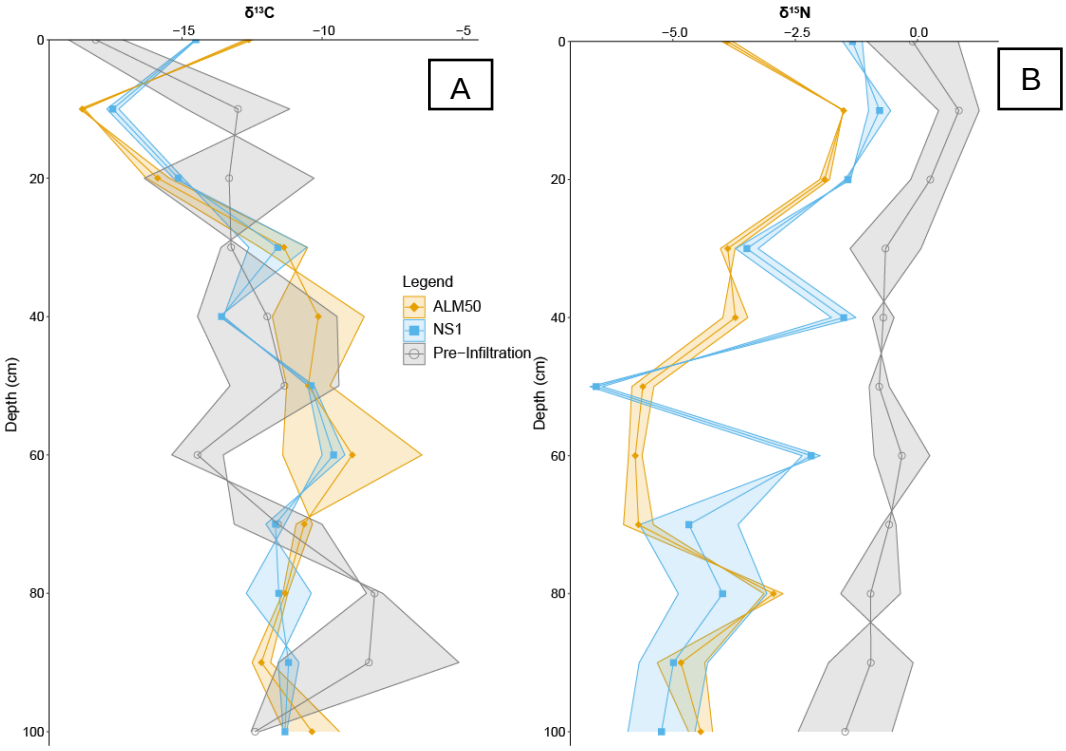

Figure 6. $\delta^{13}C$ (A) and $\delta^{15}N$ (B) soil results showing comparison between cores (native soil and almond shell 50%) and pre-infiltration soil samples in gray.

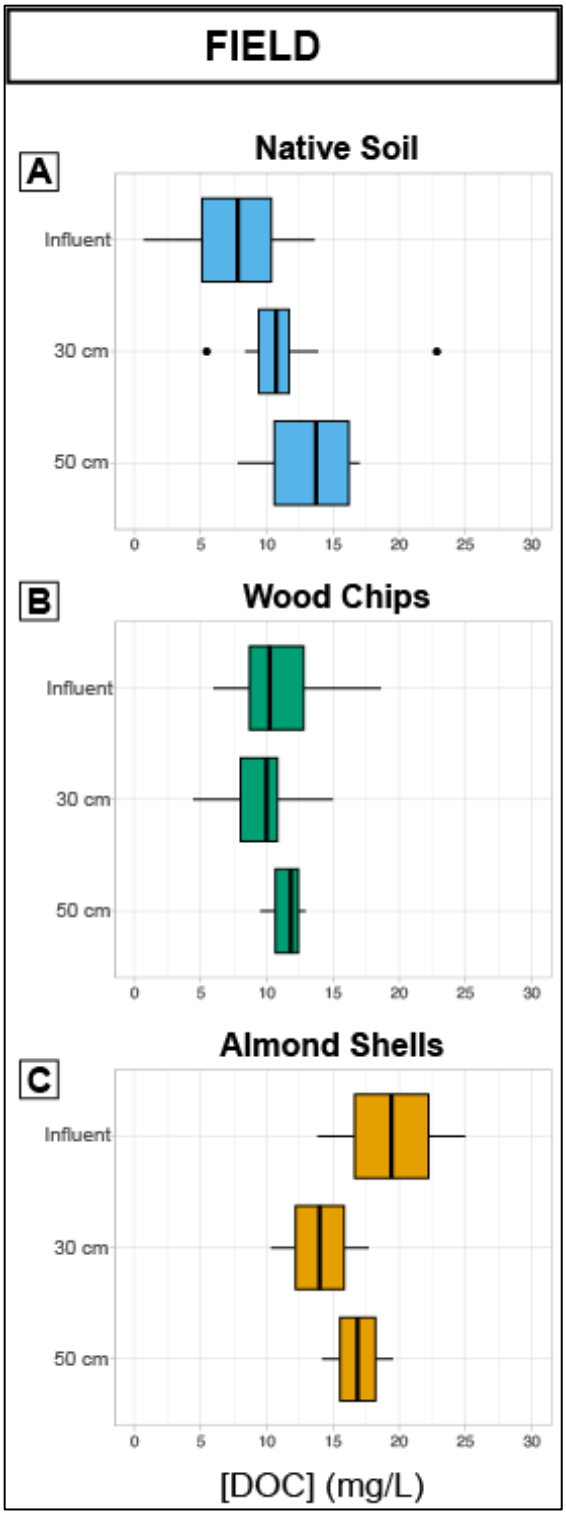

Figure 7. Field [DOC] mg/L data from WY22 and WY23. Note there is not a great deal of variation in [DOC] content among all three field treatments.

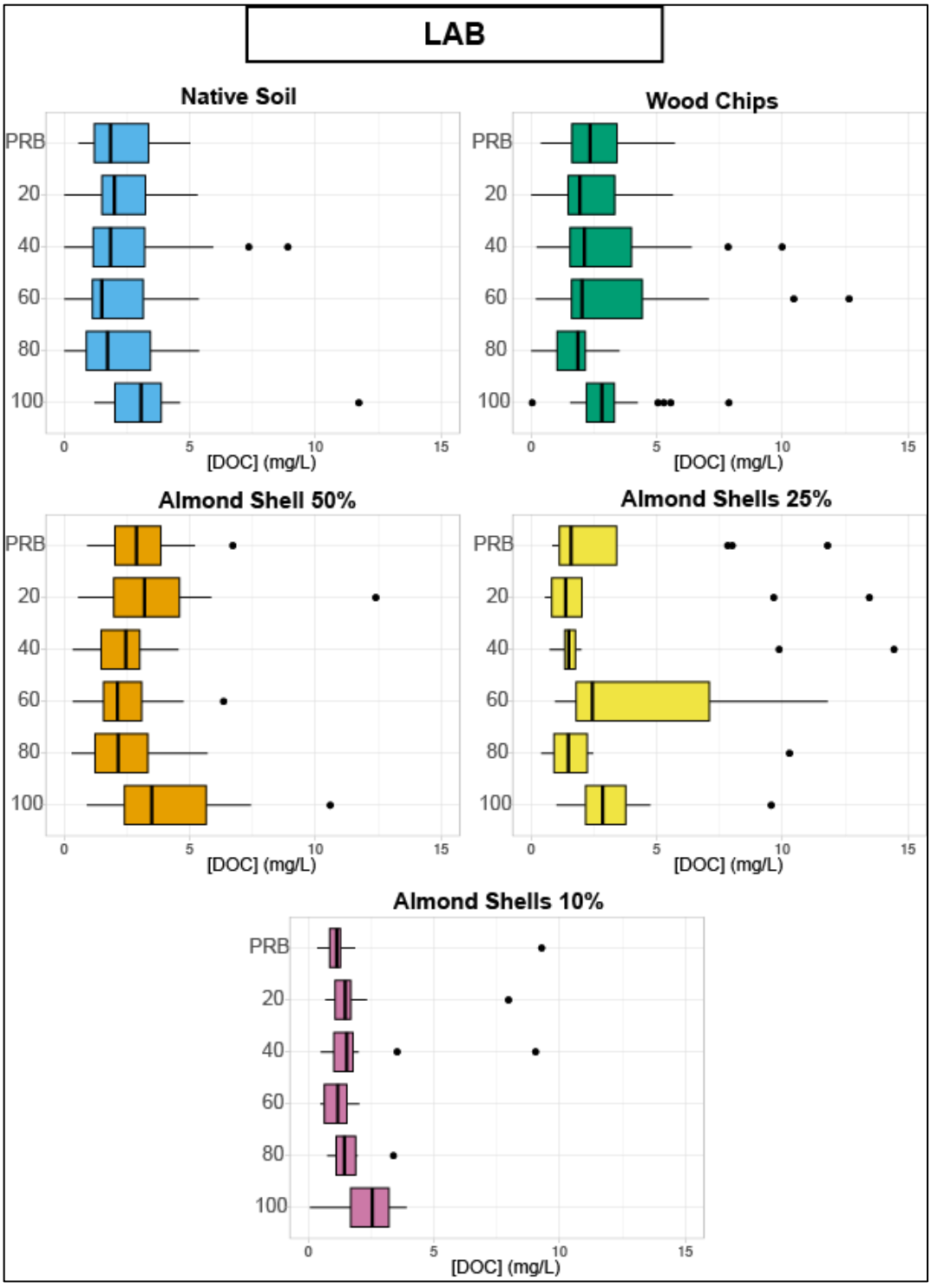

Figure 8. Lab [DOC] mg/L results by treatment and by depth. There are only slight variations in concentrations.

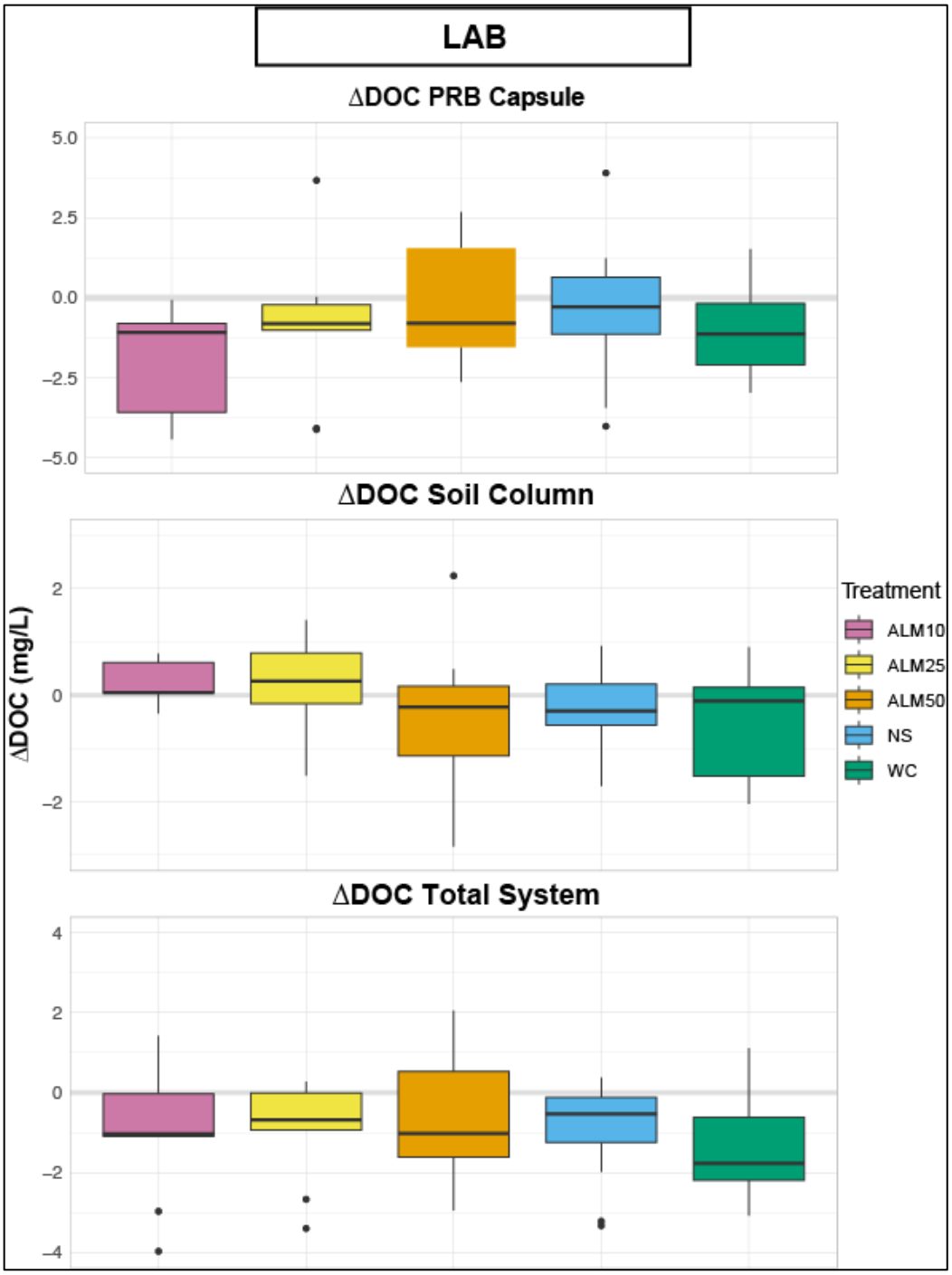

Figure 9. Lab differences in [DOC] mg/L at different locations in the lab experiments comparing all treatments. Positive values represent [DOC] gain. **(A)** Δ[DOC] within the PRB capsules: $[DOC]_{PRB} - [DOC]_{Inf} = \Delta[DOC]_{PRB}$. **(B)** Δ[DOC] within the soil cores: $[DOC]_{Eff} - [DOC]_{PRB} = \Delta[DOC]_{soil}$. **(C)** Δ[DOC] for the full experimental system: $[DOC]_{Eff} - [DOC]_{Inf} = \Delta[DOC]_{TOTAL}$.

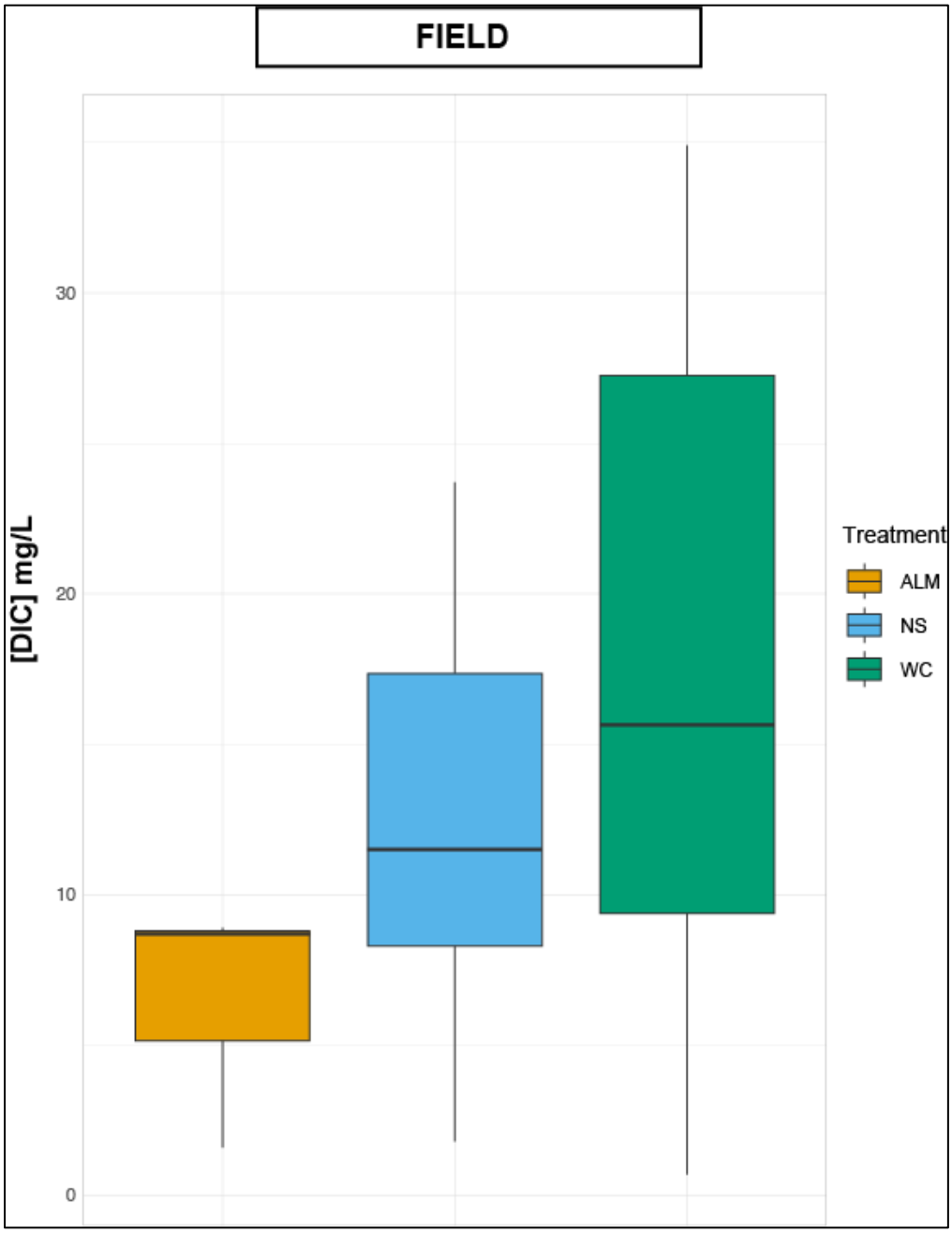

Figure 10. Field [DIC] mg/L concentrations by treatment over WY22 and WY23. The WC treatment resulted in the highest [DIC] concentrations.

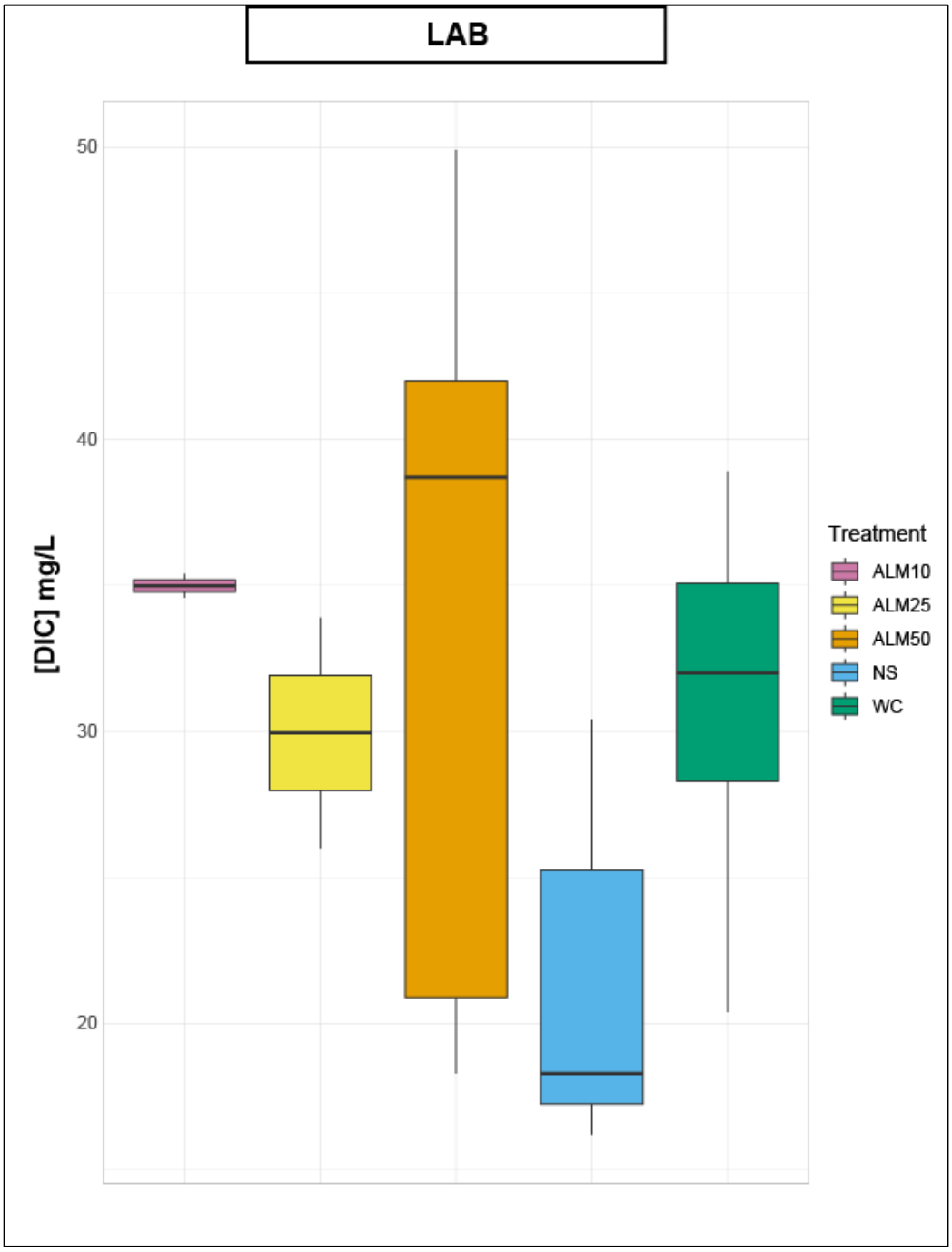

Figure 11. Lab [DIC] mg/L by treatment. The ALM50 treatment resulted in the highest concentrations, and all carbon treatments tended to be elevated relative to NS.

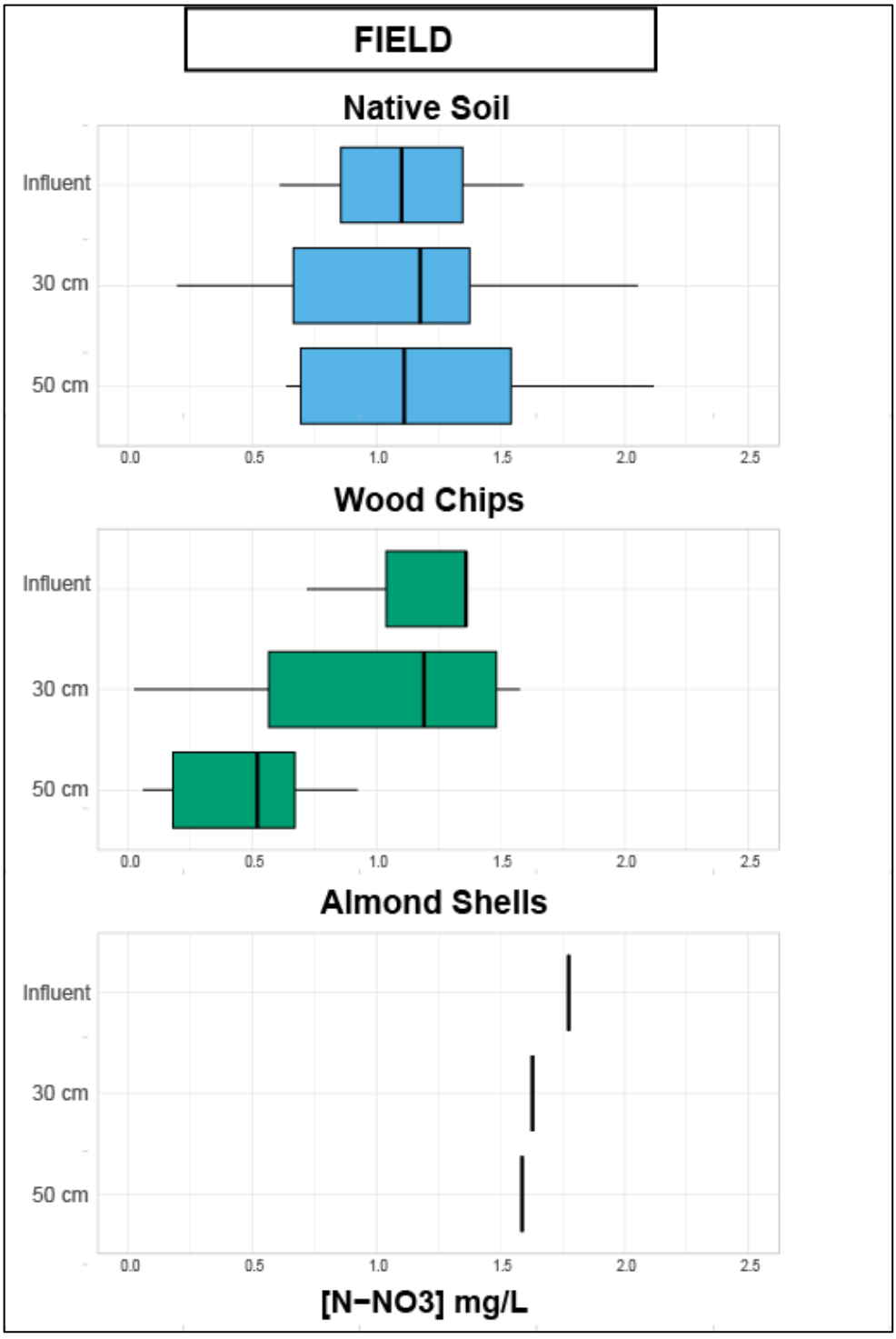

Figure 12. Field [N-NO3] mg/L data by treatment. WC removed the most nitrate in the field tests.

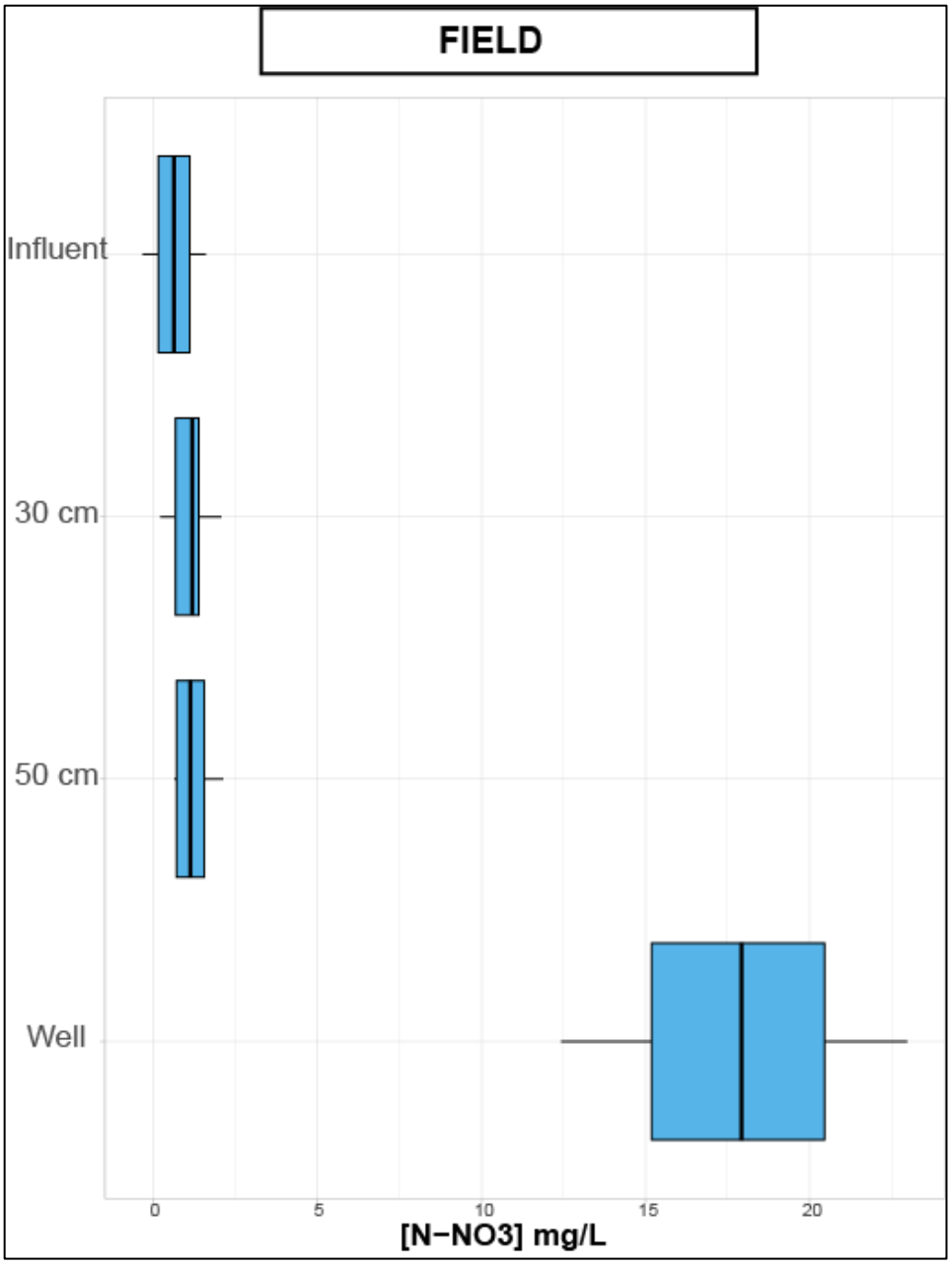

Figure 13. Field [N-NO3] mg/L data comparing basin shallow subsurface samples shallow farm well [N-NO3] values.

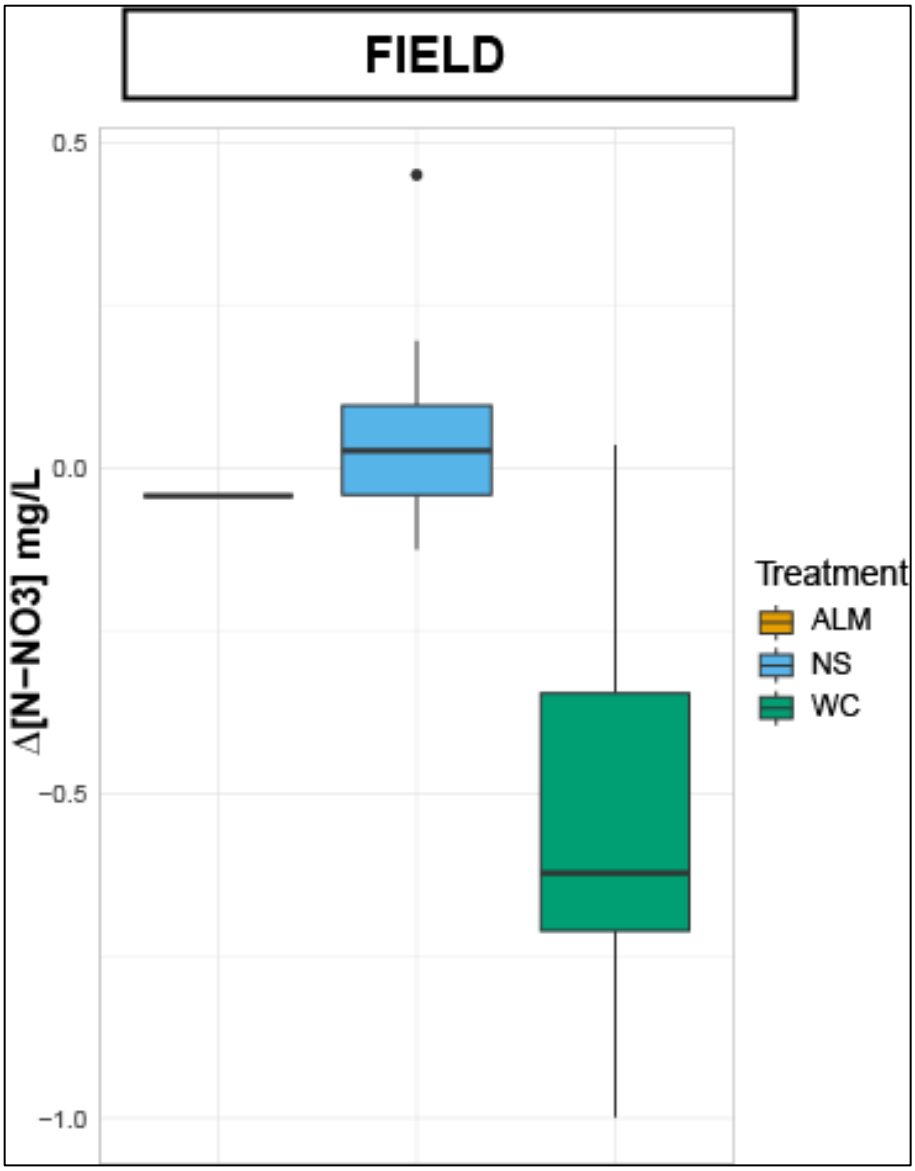

Figure 14. Field △[N-NO3] ([N-NO3]$_{30\ cm\text{-}bgs}$ - [N-NO3]$_{50\ cm\text{-}bgs}$ by treatment.

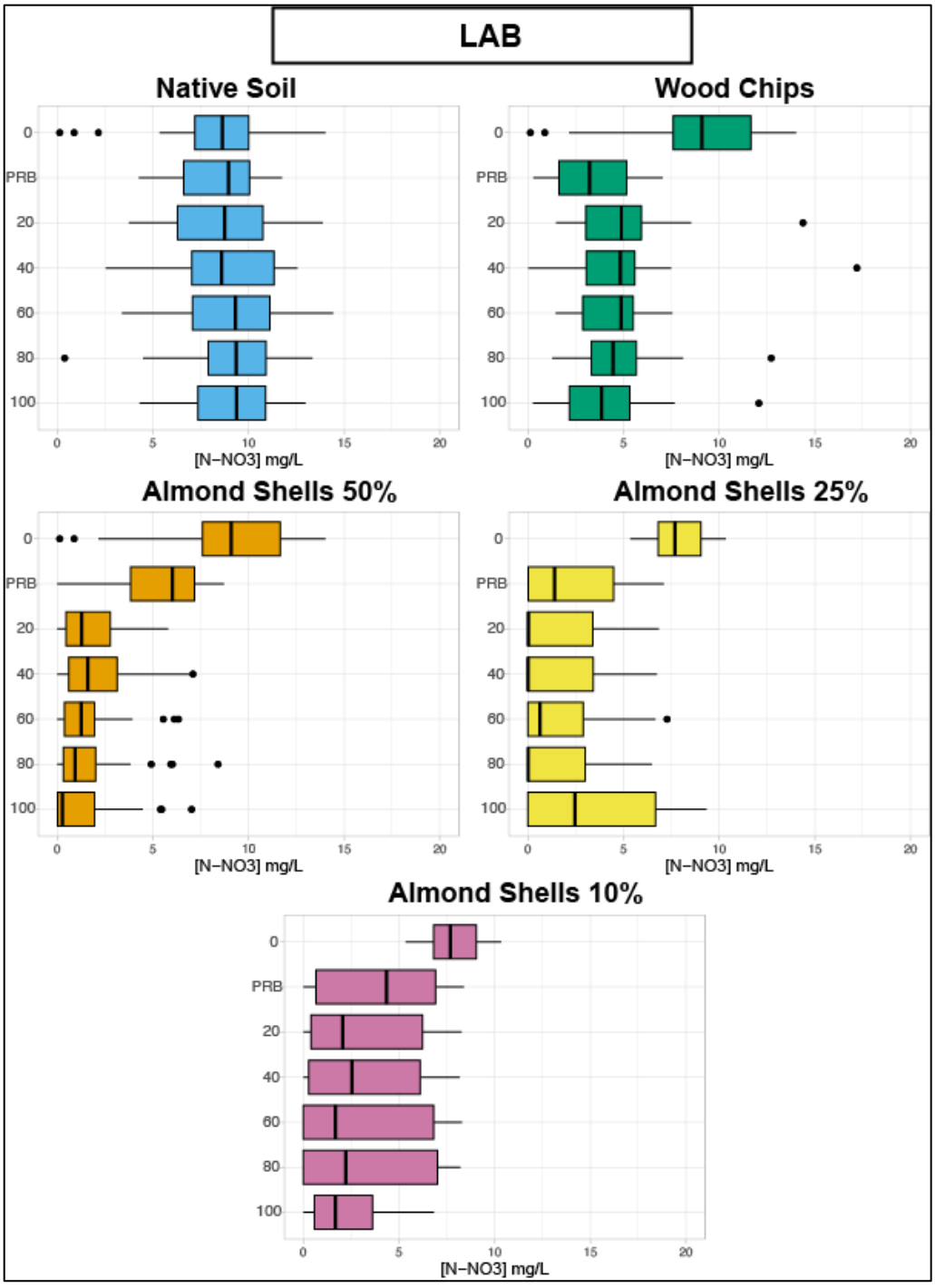

Figure 15. Lab [N-NO3] mg/L by treatment and depth. ALM50 and ALM25 removed the most nitrate.

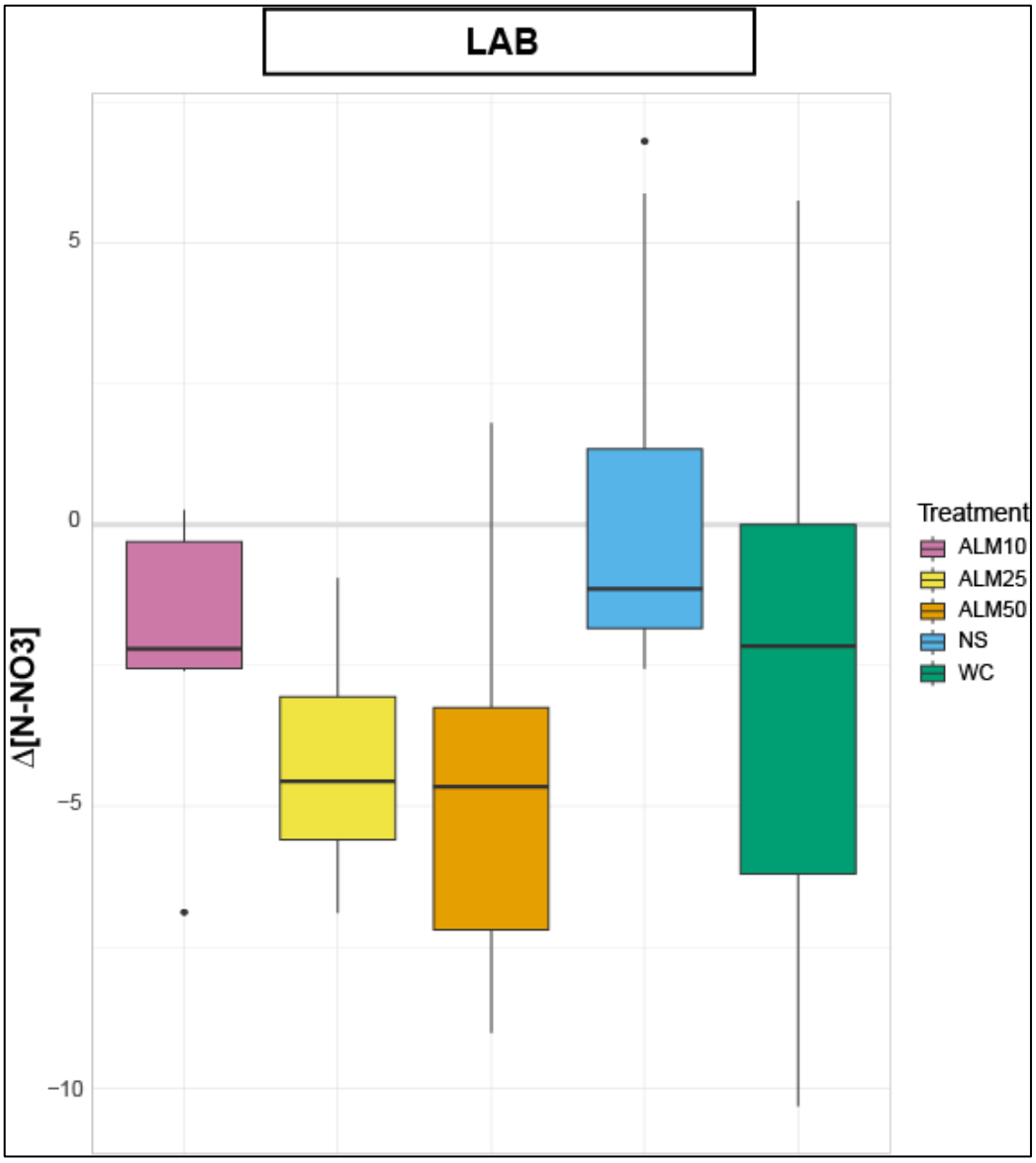

Figure 16. Δ[N-NO_3] mg/L each treatment in the PRB capsule: [N-NO_3]$_{PRB}$ – [N-NO_3]$_{Inf}$.

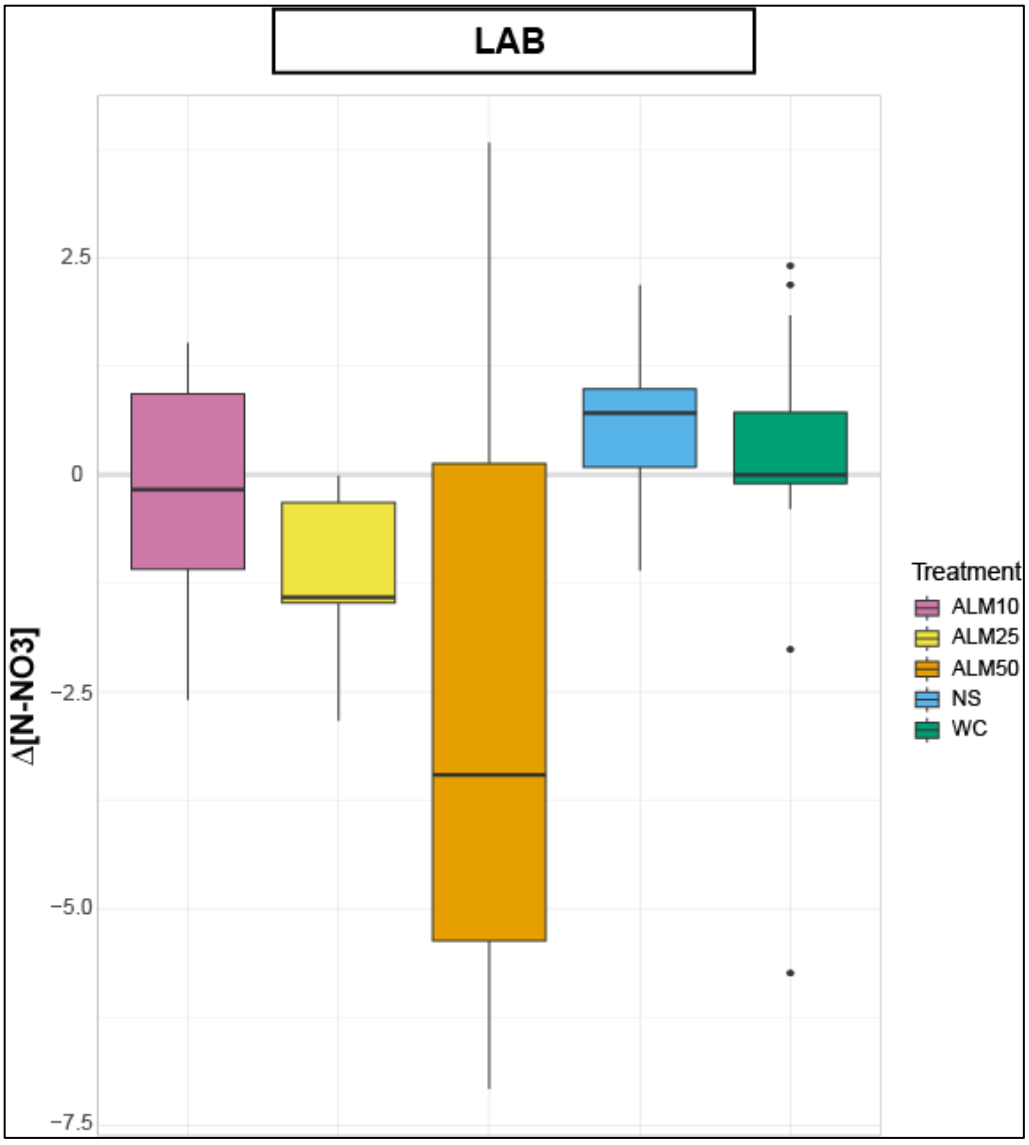

Figure 17. Δ[N-NO_3] (mg/L) during flow through soil cores during laboratory experiments: $[N\text{-}NO_3]_{Eff} - [N\text{-}NO3]_{PRB}$. Negative values indicate net NO_3 removal.

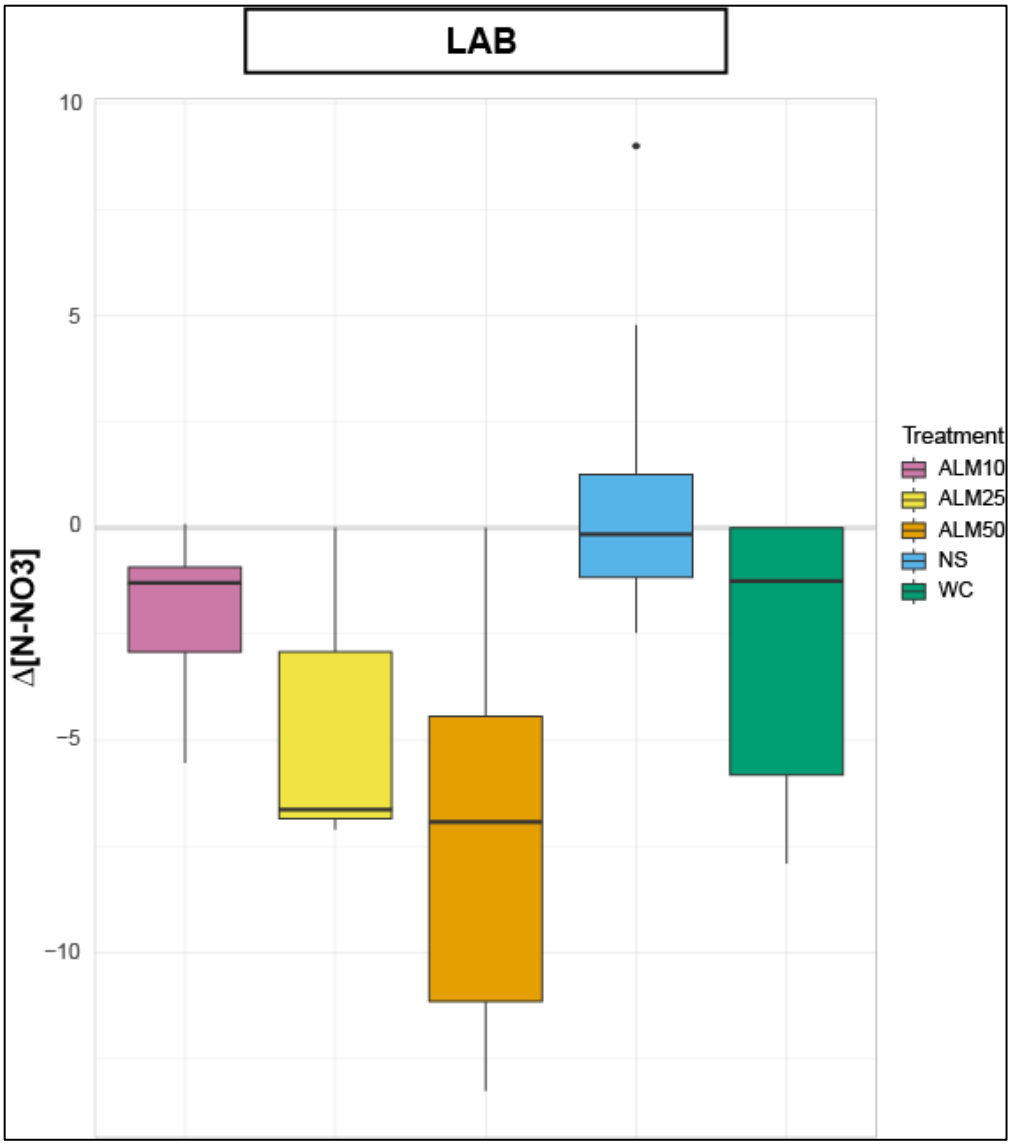

Figure 18. Δ[N-NO_3] (mg/L) during flow through PRBs and soil cores during laboratory experiments: [N-NO_3]$_{Eff}$ – [N-NO3]$_{INF}$. Negative values indicate net NO_3 removal.

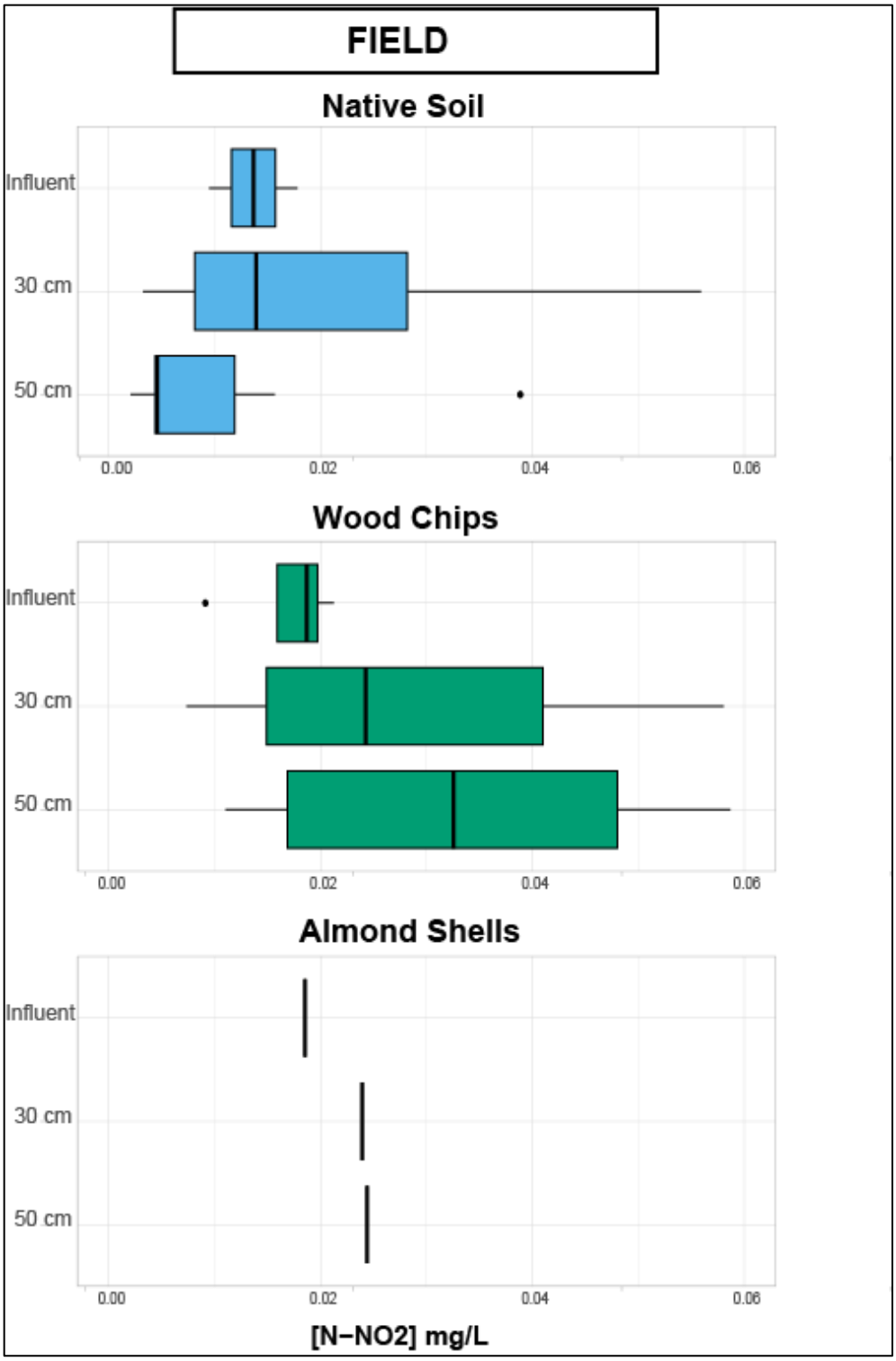

Figure 19. Field [N-NO2] mg/L data by treatment.

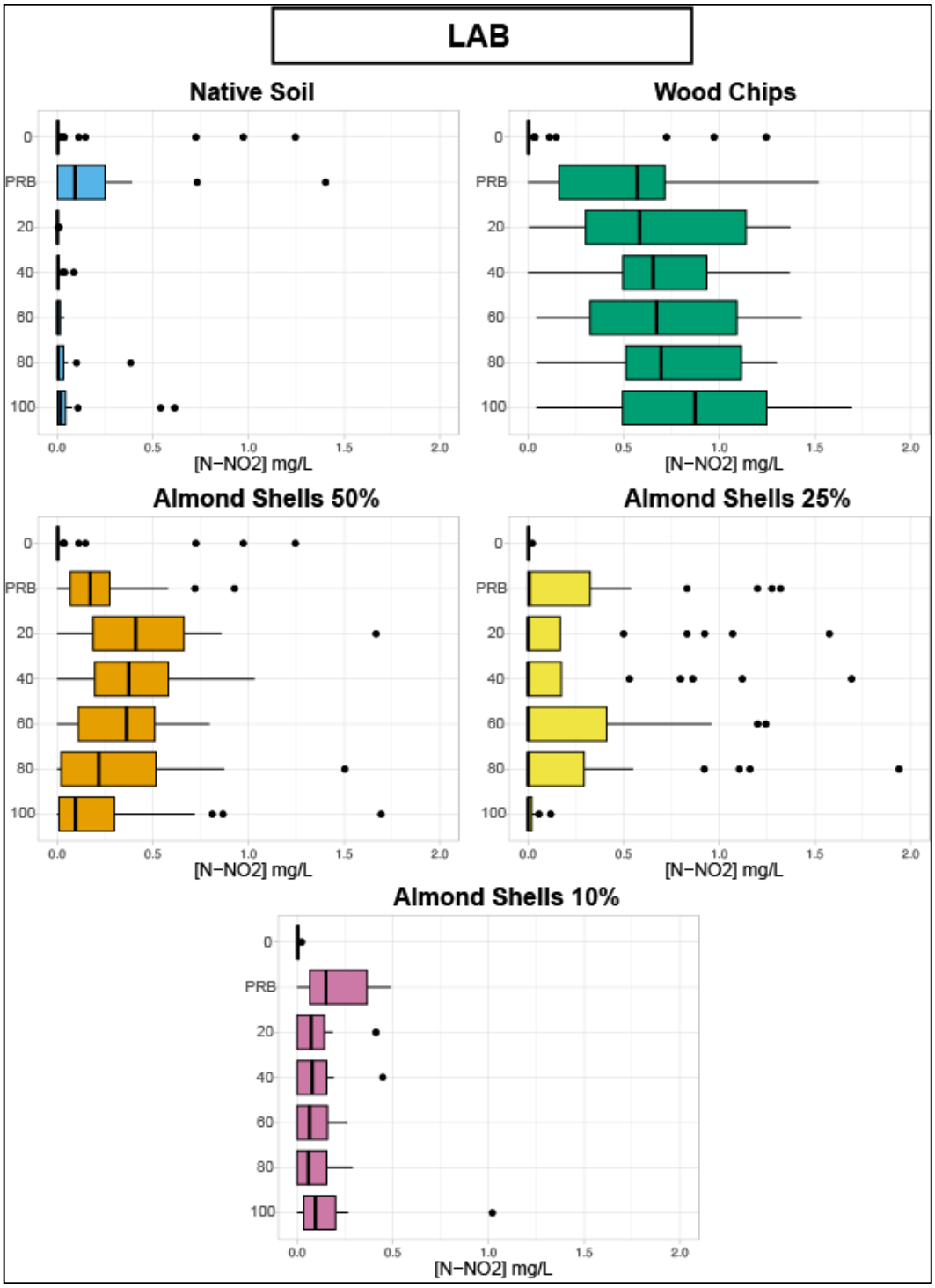

Figure 20. [N-NO2] mg/L by treatment and depth.

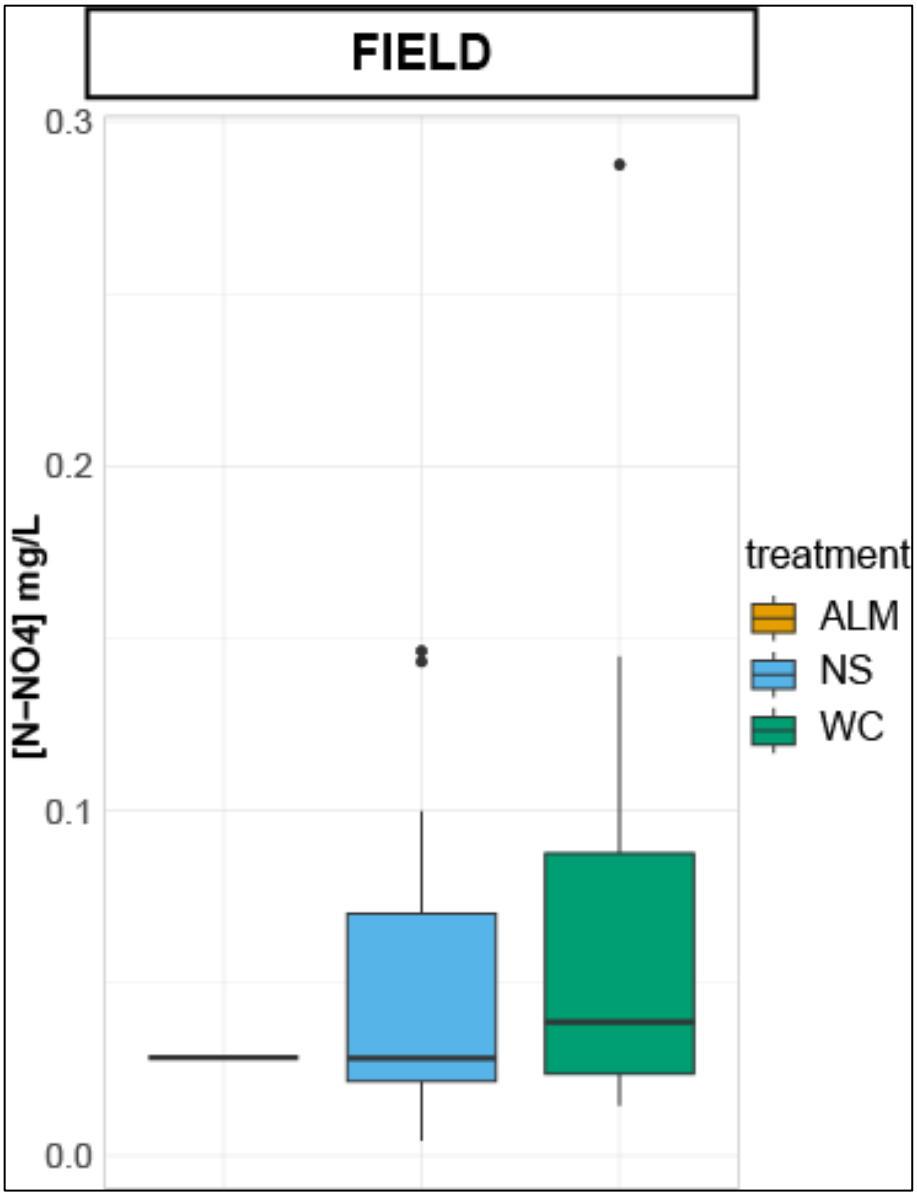

Figure 21. Field [N-NH4] mg/L by treatment.

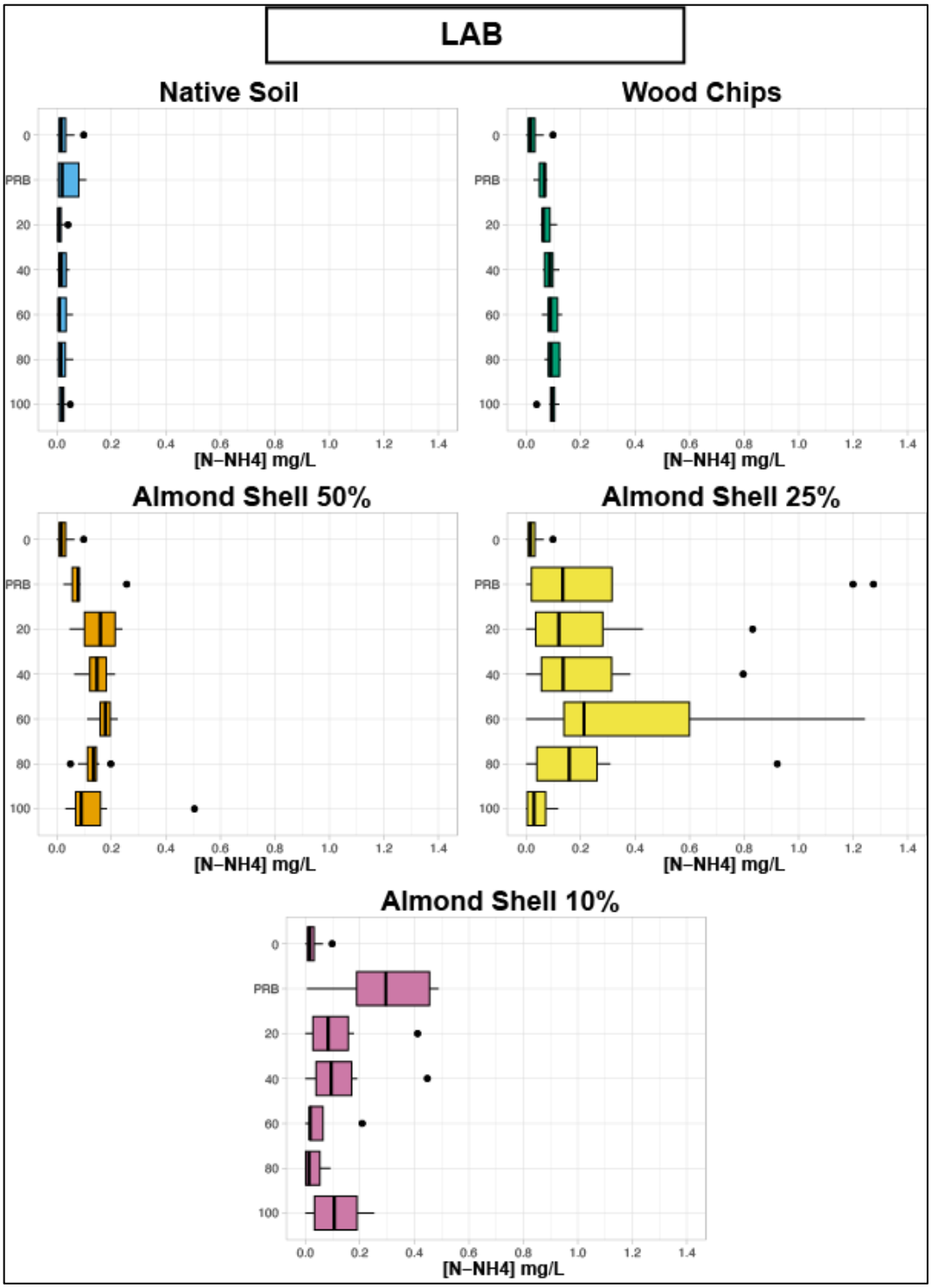

Figure 22. [N-NH4] mg/L by treatment and depth.

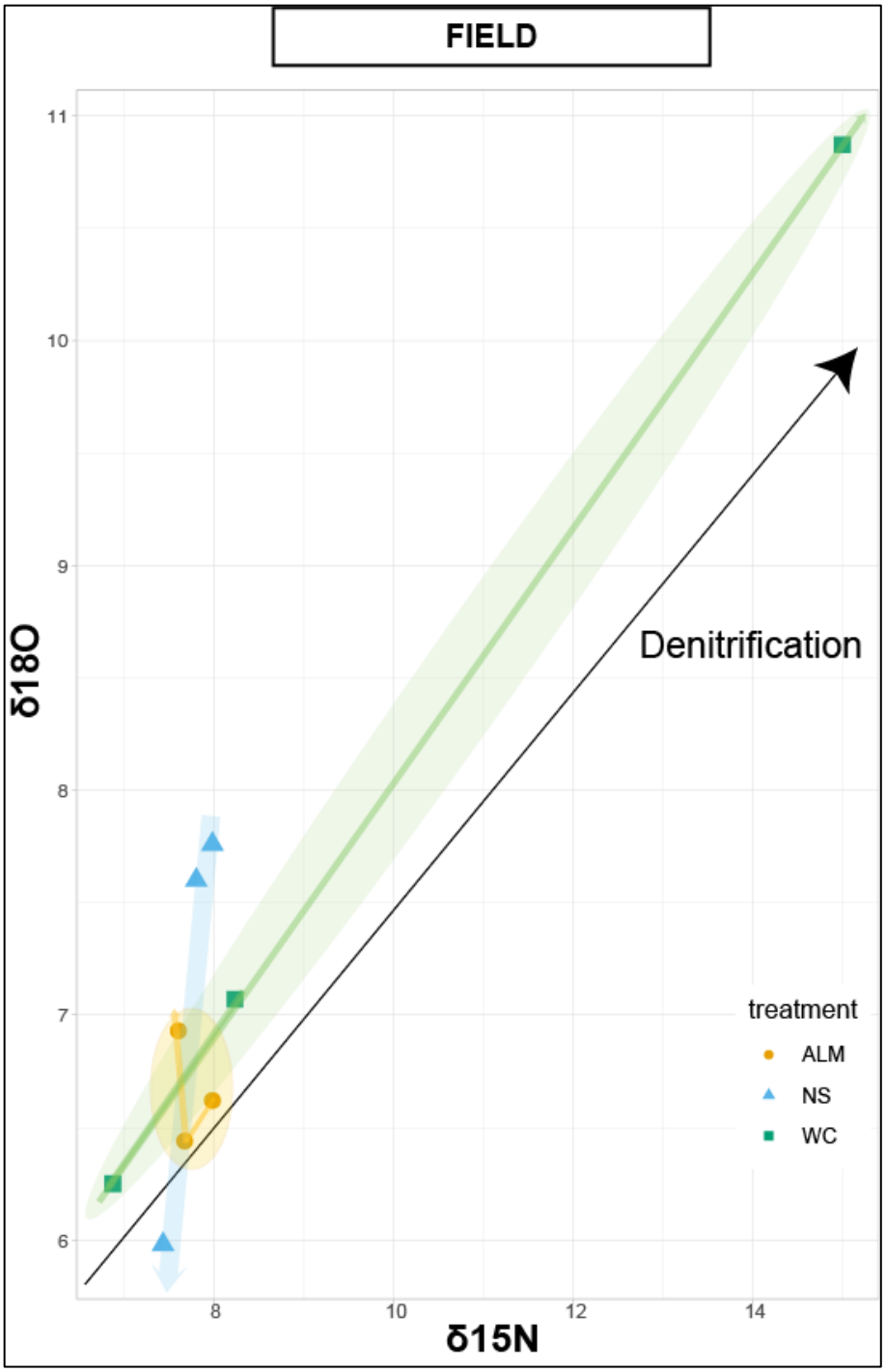

Figure 23. Isotopes of nitrate cross plot for KTR field treatments. Approximate 2:1 denitrification slope shown in black. Arrows show approximate path from influent – 30 cm-bgs – 50 cm-bgs (colors associated with each treatment).

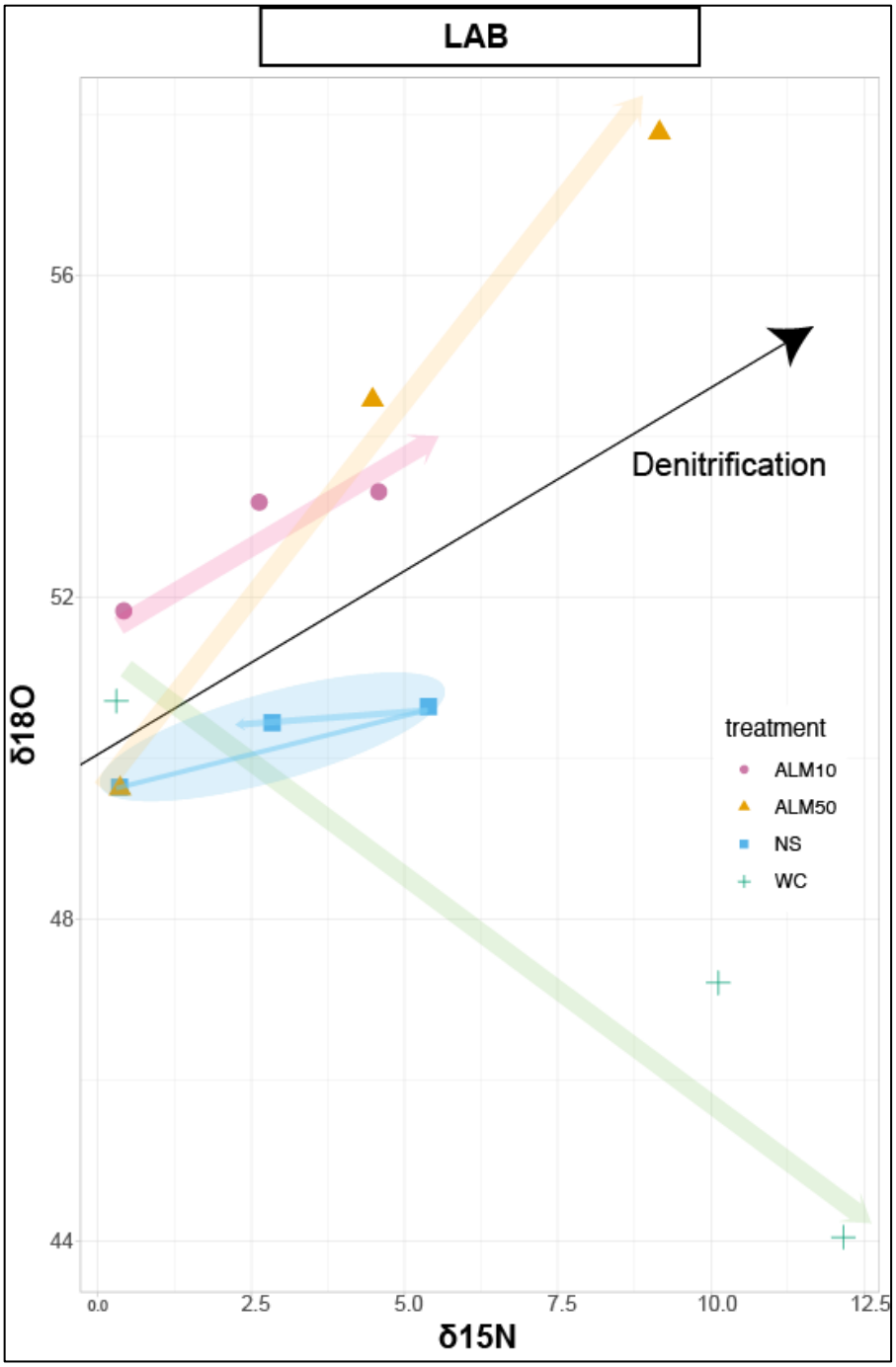

Figure 24. Isotopes of nitrate cross plot for cores. Approximate 2:1 denitrification slope shown in black. Arrows show approximate path from influent – PRB – effluent (colors associated with each treatment).

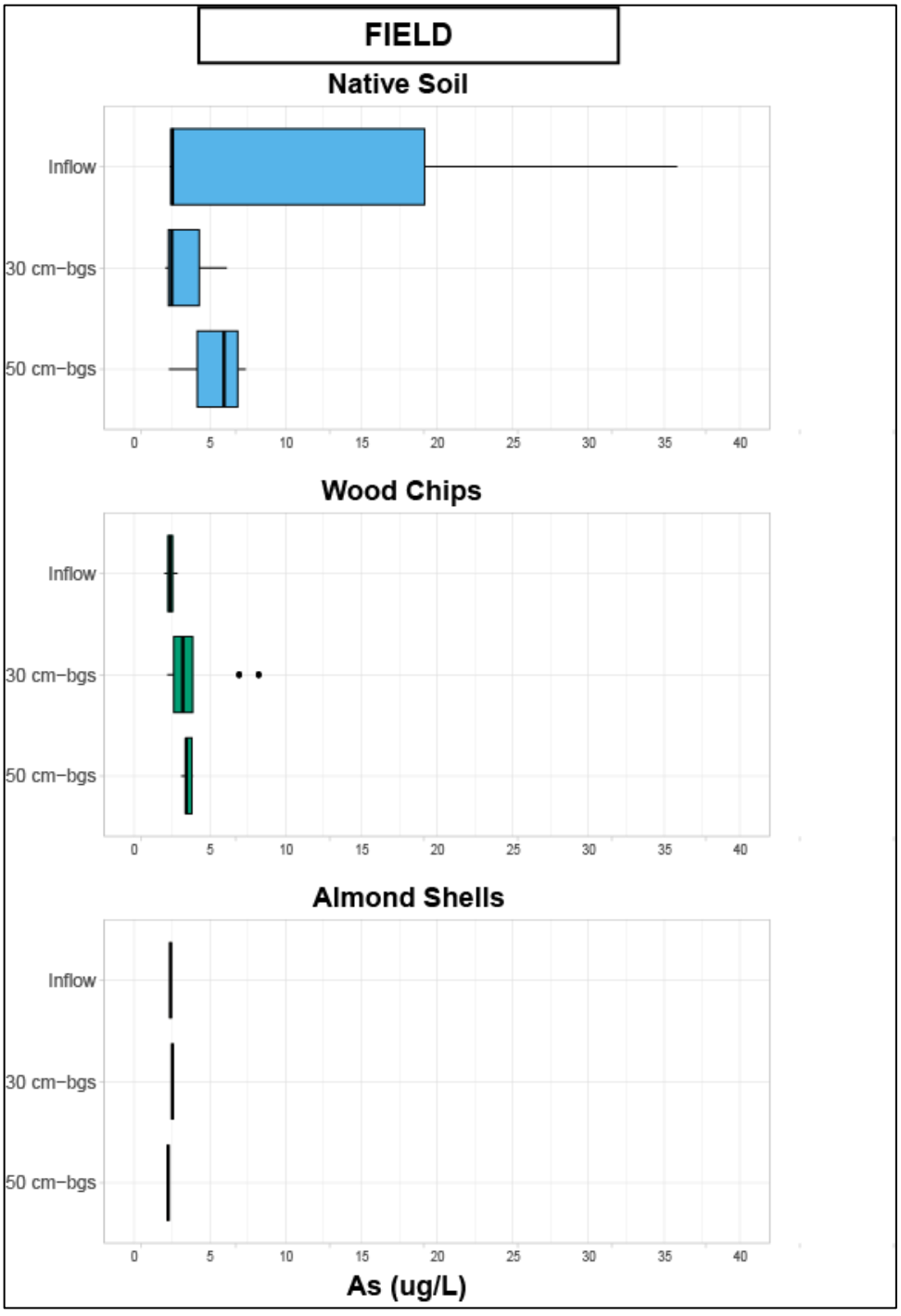

Figure 25. Depth plots comparing arsenic concentrations in ug/L by treatment in KTR field samples.

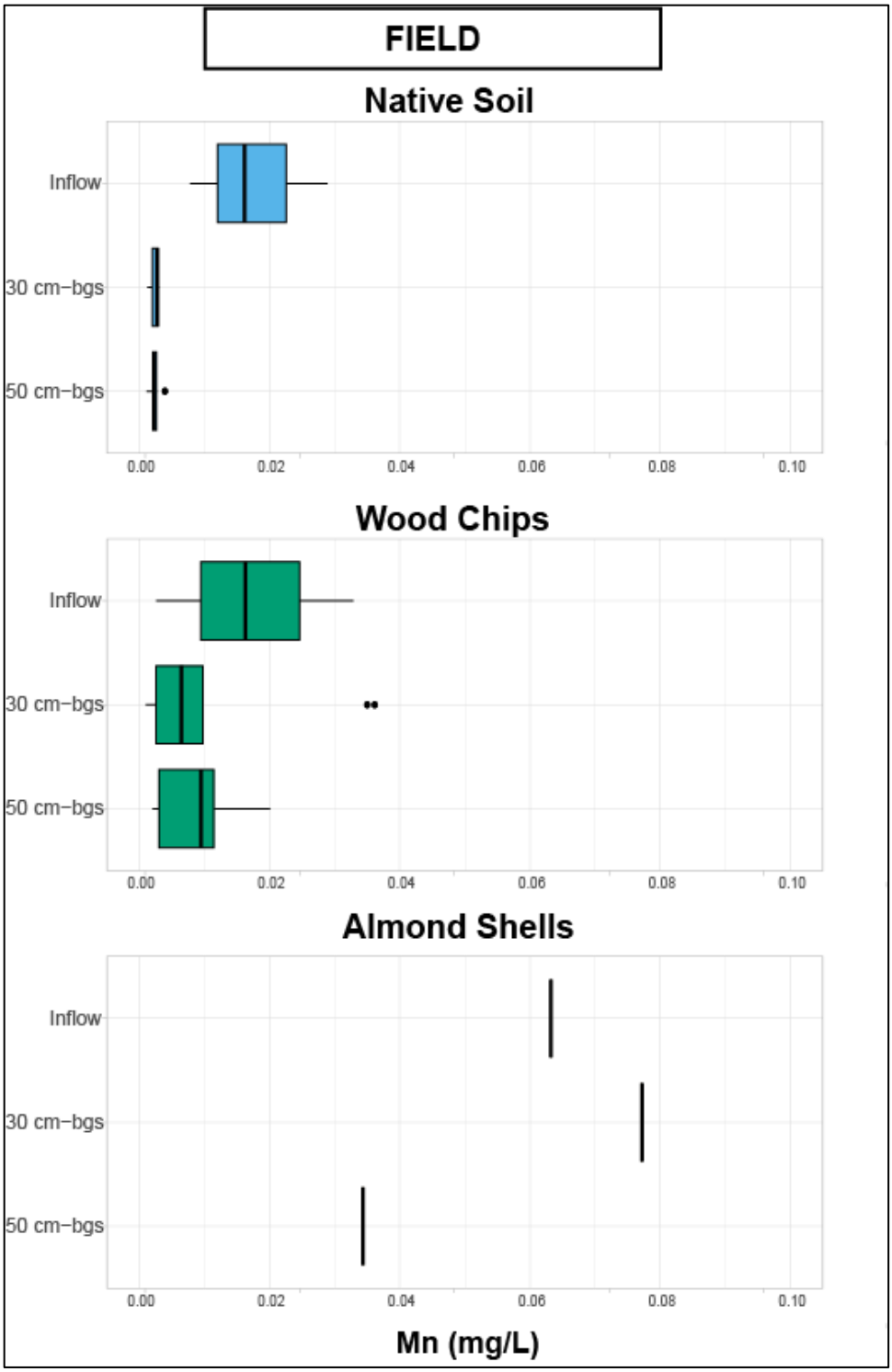

Figure 26. Depth plots comparing manganese concentrations in ug/L by treatment in KTR field samples.

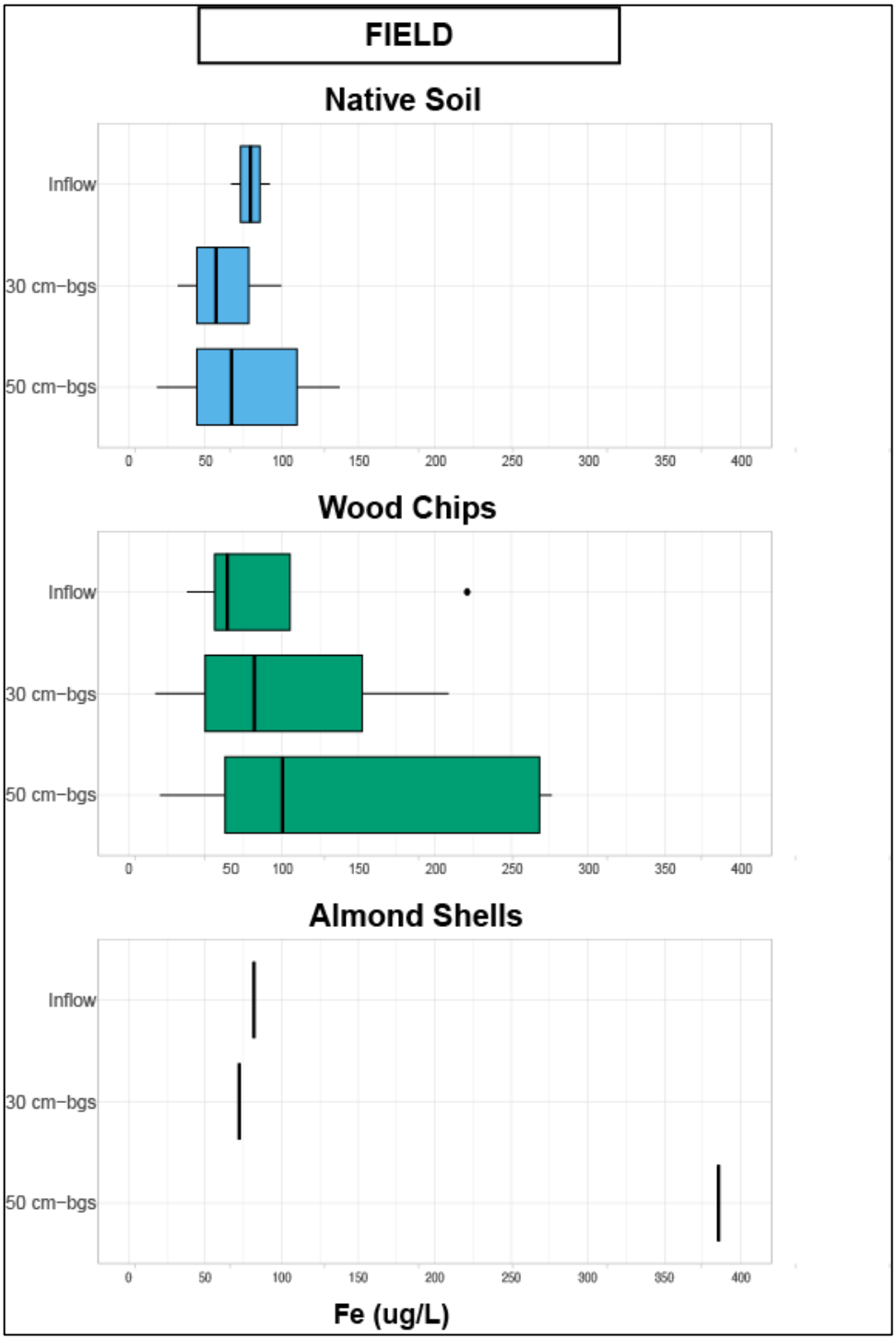

Figure 27. Depth plots comparing iron concentrations in ug/L by treatment in KTR field samples.

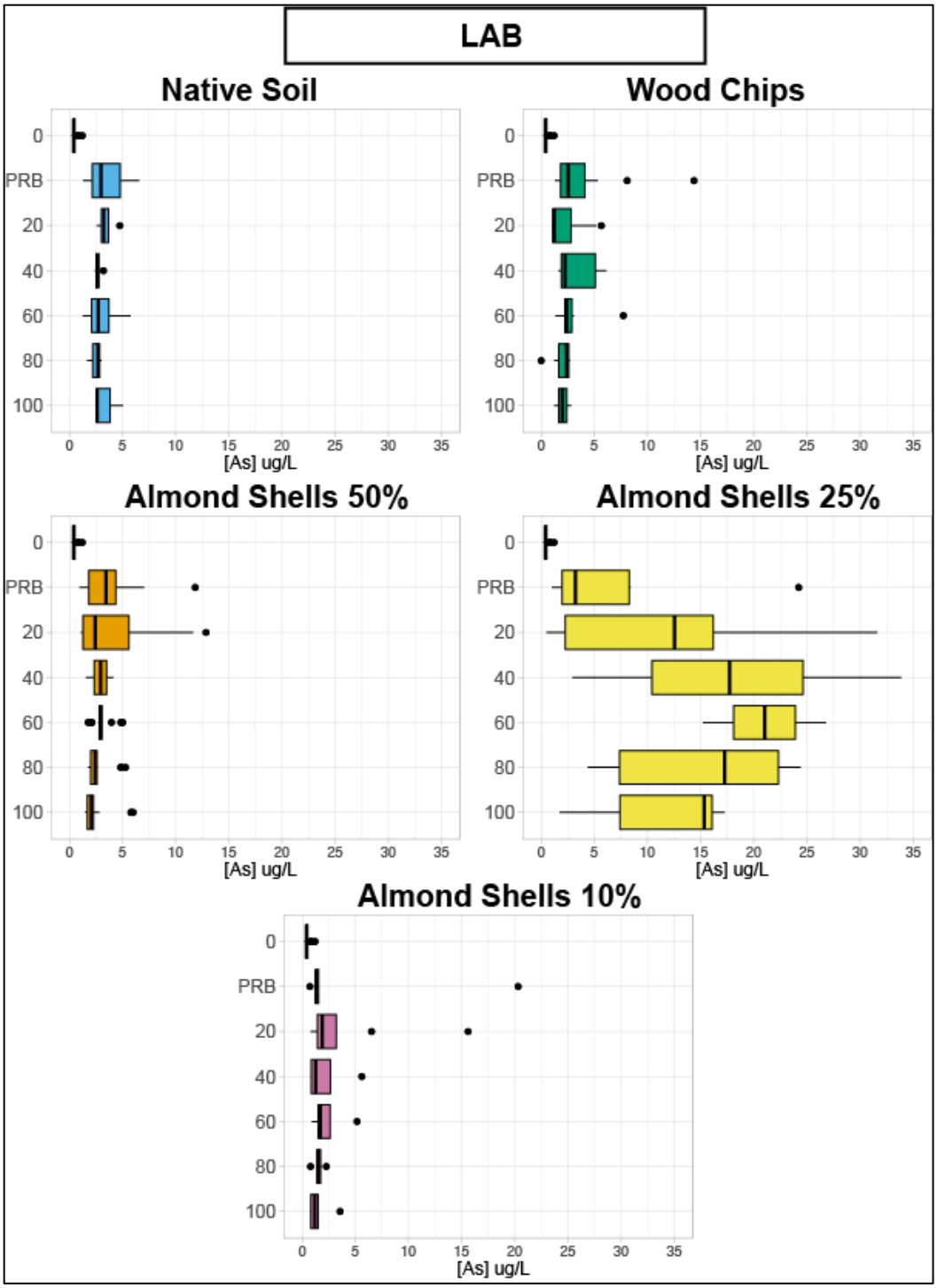

Figure 28. Depth plots comparing arsenic concentrations in ug/L by treatment.

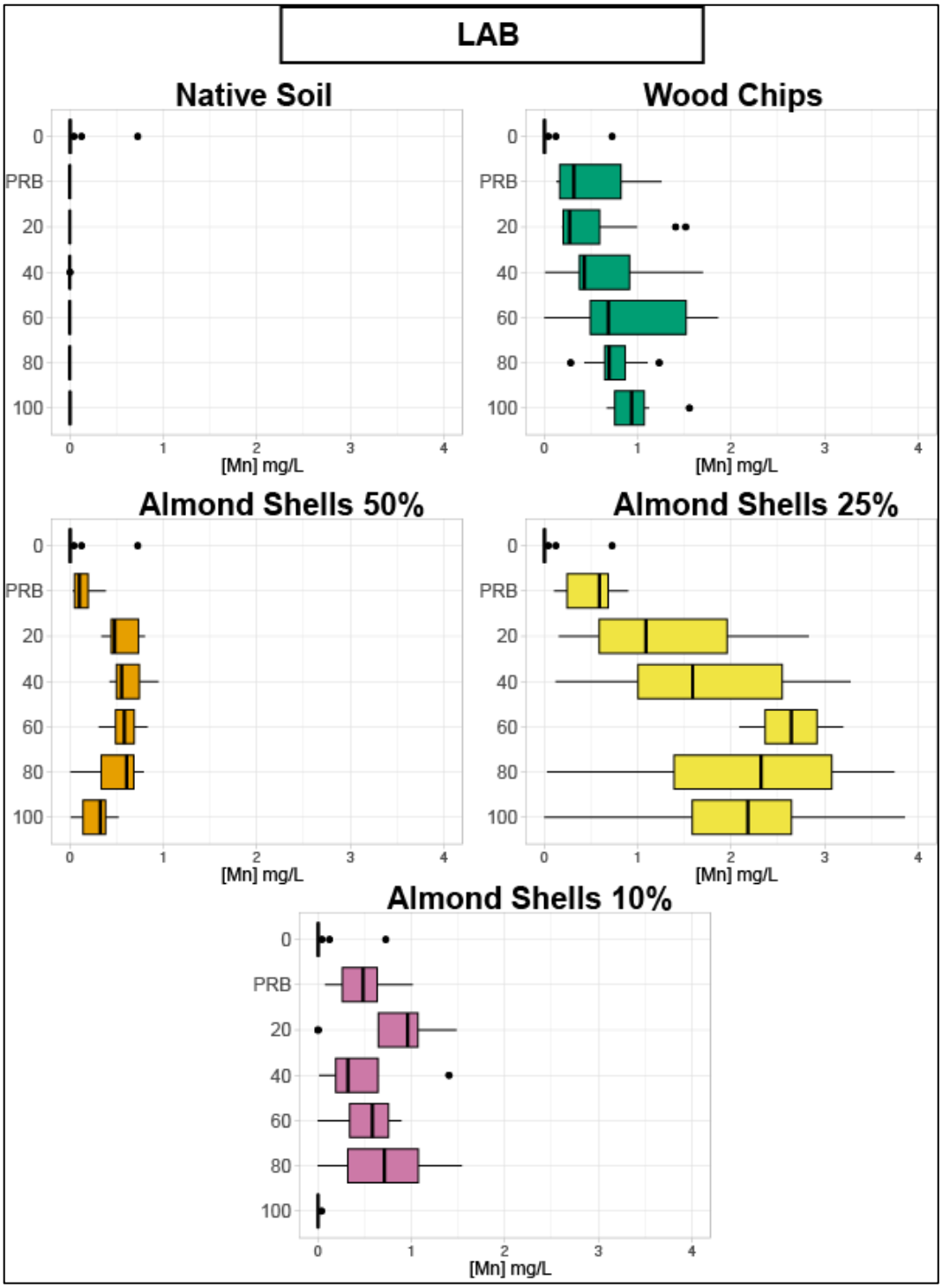

Figure 29. Depth plots comparing manganese concentrations in mg/L by treatment.

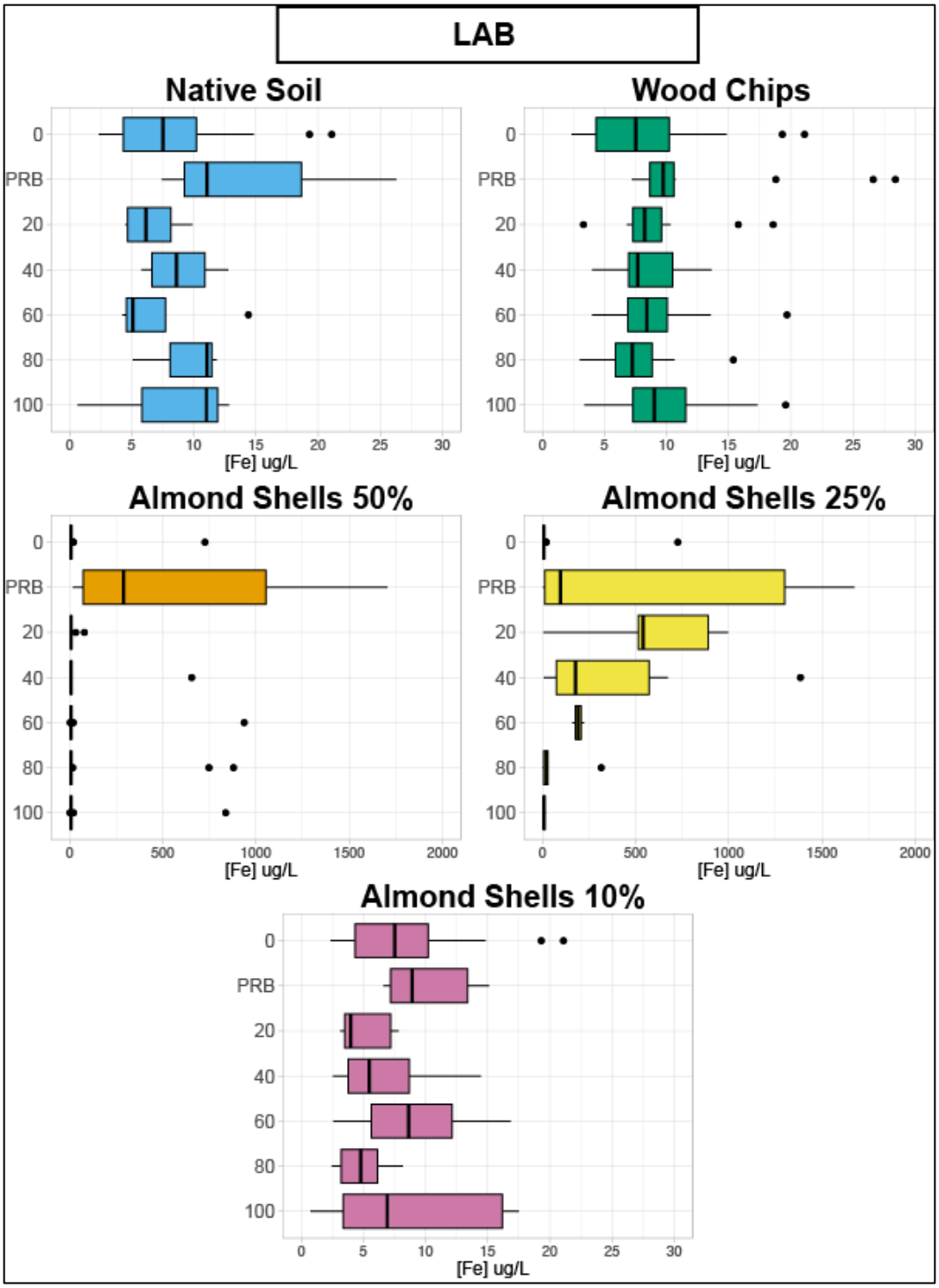

Figure 30. Depth plots comparing iron concentrations in mg/L by treatment. Note the differing x-axis scales on almond shell 50% and almond shell 25%.

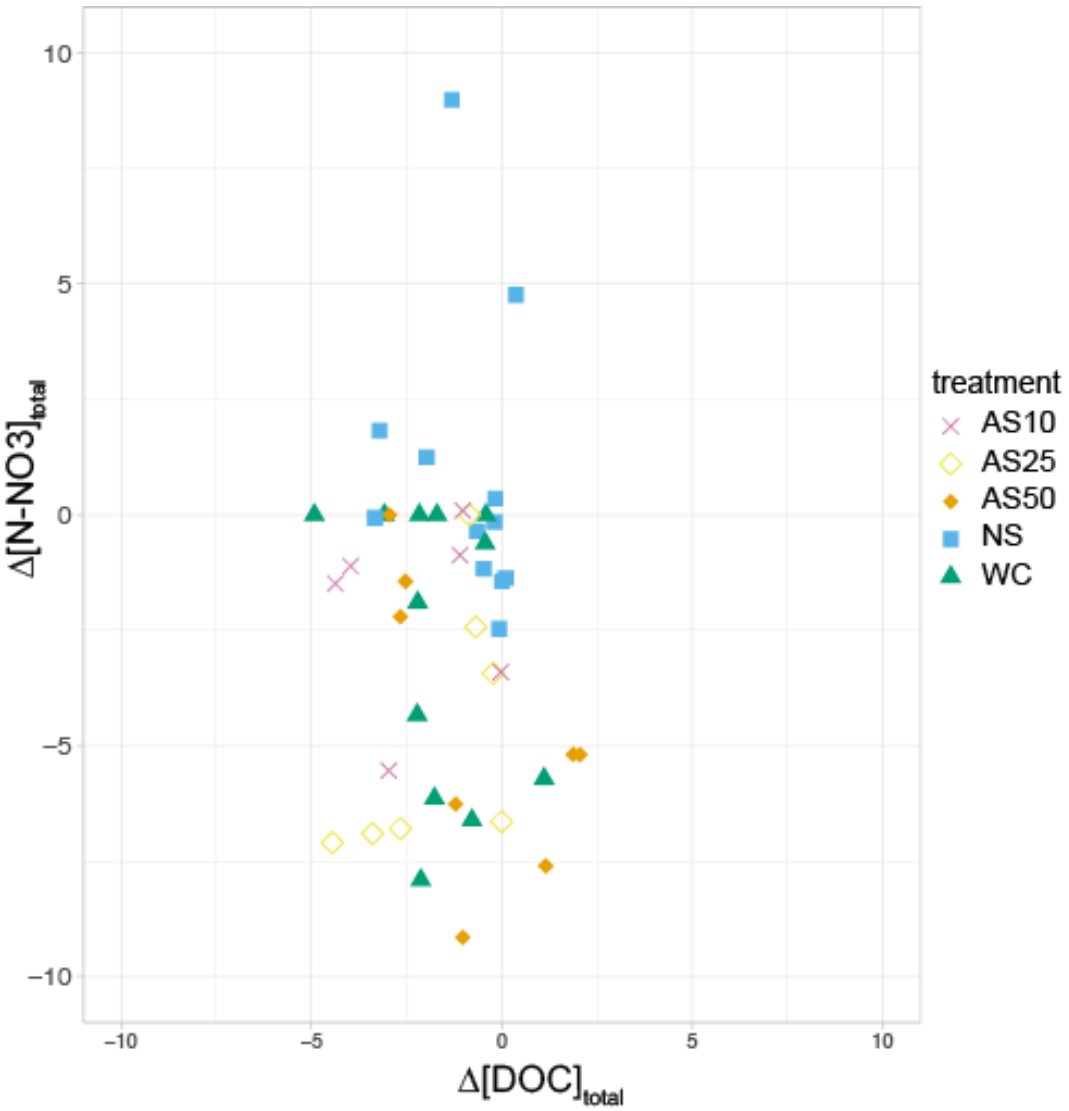

Figure 30. $\Delta[DOC]_{total}$ vs $\Delta[N\text{-}NO3]_{total}$ for all five lab treatments.

Table 1. KTR Treatment history (WY22-WY23). Note, there were no additional treatments added in WY21 or WY23.

Site Code	Number of subsurface samples collected in WY22	Number of subsurface samples collected in WY23	WY20 Treatment	WY22 Treatment
03A	3	NA[a]	Native soil	Native soil
05A	NA[a]	6	Native soil	Native Soil
05A'	NA[a]	6	Native soil	Native Soil
16A	4	NA[a]	Almond shells	Native Soil
15A	4	NA[a]	Almond shells	Almond shells & rice husks
14A	4	6	Wood mulch & alfalfa	Wood chips
14A'	NA[a]	6	Wood mulch & alfalfa	Wood chips
10A	3	NA[a]	Biochar & wood mulch	Wood chips
11A	4	NA[a]	Biochar	Wood chips
14C	4	NA[a]	Wood mulch	Wood chips

[a] Piezometer location not installed that water year

Table 2. Key name codes for cores and augered samples with treatment type and ratio of native soil to treatment PRB capsules.

Name Code	Pre or Post	Collection Method	Treatment Type	PRB Capsule composition Native soil:treatment
AUG[a]	Pre	Hand augered	Native soil	NA
NS	Post	Cored	Native soil	50:50
WC	Post	Cored	Wood chips	50:50
ALM50	Post	Cored	Almond shells	50:50
ALM25	Post	Cored	Almond shells	75:25
ALM10	Post	Cored	Almond shells	90:10

[a] samples not used in flow through experiments, referred to as pre-infiltration samples. Post infiltration samples are cores used in infiltration experiences that were measured after experiments ran.

Table 3. Grain size composition and distribution. NS1 and NS2 represent two separate control cores in the two separate infiltration experiments. In other results, NS1 and NS2 have been aggregated.

Core ID	Samples Analyzed (n)	Avg d_{50} (μm)	Mean absolute deviation (MAD)	Standard deviation	Mean grain size (μm)
NS1[a]	16	268	15.9	41.0	315
NS2[a]	17	258	19.3	39.3	304
WC	14	273	39.5	58.1	321
ALM10	15	264	14.4	18.7	317
ALM25	14	256	21.1	47.3	309
ALM50	14	277	42.9	51.5	328

[a] samples not used in flow through experiments, referred to as “pre-infiltration”

Table 4. Median ± standard deviation for concentrations of carbon (A) and nitrogen (B) and isotopes of carbon and nitrogen. (Note that wood chips were not analyzed in this portion of the study).

A.

Core ID	Samples Analyzed (n)	Median [C] (ppm) ± MAD	Mean [C] (ppm) ± SD	Median $\delta^{13}C$ ‰ ± MAD	Mean $\delta^{13}C$ ‰ ± SD
AUG	22	2400 ± 297	2354 ± 430	-12.7 ± 3.38	-12.3 ± 3.27
NS	22	2250 ± 371	2332 ± 610	-11.8 ± 2.15	-12.5 ± 2.35
ALM50	22	2050 ± 518	2159 ± 497	-11.4 ± 1.59	-12.0 ± 2.94

B.

Core ID	Samples Analyzed (n)	Median [N] (ppm)	Mean [N] (ppm)	Median $\delta^{15}N$‰	Mean $\delta^{15}N$ ‰
AUG	22	125 ± 15	135 ± 28	-0.5 ± 0.76	-0.49 ± 0.89
NS	22	170 ± 30	179 ± 37	-3.17 ± 2.53	-3.29 ± 1.98
ALM50	22	175 ± 22	178 ± 31	-4.02 ± 1.91	-4.02 ± 1.45

Table 5. Pairwise Willcox Test P-value results for [DOC] mg/L coming off of the PRB capsule among all 5 treatments types.

	WC	ALM50	ALM25	ALM10
NS	0.80	0.86	0.87	0.80
ALM10	0.86	0.80	0.80	
ALM25	0.80	0.86		
ALM50	0.80			

Table 6. Pairwise Willcox Test P-value results for [DOC] mg/L changes in the soil core among all 5 treatment types.

	WC	ALM50	ALM25	ALM10
NS	0.99	0.99	0.92	0.92
ALM10	0.92	0.92	0.99	
ALM25	0.92	0.92		
ALM50	1.0			

Table 7. Pairwise Willcox Test P-value results for [DOC] mg/L total change among all 5 treatment types.

	WC	ALM50	ALM25	ALM10
NS	0.85	0.95	0.95	0.95
ALM10	0.95	0.95	0.85	
ALM25	0.85	0.95		
ALM50	0.85			

Table 8. Pairwise Willcox Test P-value results for [DIC] mg/L data among all 5 treatment types.

	WC	ALM50	ALM25	ALM10
NS	**0.00048**[a]	**0.033**[a]	0.216	0.10
ALM10	0.56	0.93	0.56	
ALM25	0.88	0.93		
ALM50	0.88			

[a] p-values are < 0.05 meaning these two treatments' populations are significantly different from each other

Table 9. Pairwise Willcox Test P-value results for [N-NO3] mg/L removed only in the PRB capsule among all 5 treatment types.

	WC	ALM50	ALM25	ALM10
NS	0.26	**0.0079**[a]	**0.024**[a]	0.26
ALM10	0.64	0.26	0.26	
ALM25	0.43	0.64		
ALM50	0.29			

[a] p-values are < 0.05 meaning these two treatments' populations are significantly different from each other

Table 10. Pairwise Willcox Test P-value results for [N-NO3] mg/L removed only in the soil core among all 5 treatment types.

	WC	ALM50	ALM25	ALM10
NS	0.33	**0.068**[b]	**0.012**[a]	0.33
ALM10	0.58	0.26	0.33	
ALM25	0.082	0.33		
ALM50	0.17			

[a] p-values are < 0.05 meaning these two treatments' populations are significantly different from each other

[b]This value is above the p-value cut off, but upon visual inspection, we determine that ALM50 is significantly different than NS.

Table 11. Pairwise Willcox Test P-value results for [N-NO3] mg/L removal data among all 5 treatment types.

	WC	ALM50	ALM25	ALM10
NS	0.12	**0.0024**[a]	**0.012**[a]	0.12
ALM10	0.81	**0.070**[a]	0.12	
ALM25	0.15	0.39		
ALM50	0.067			

[a] p-values are < 0.05 meaning these two treatments' populations are significantly different from each other

Table 12. Mean and median values of [N-NO3] removed for every treatment in three different situations: the total amount from influent to effluent (A), only in the PRB capsule (B), and only in the soil core (C). ALM50 values shown in bold because they are the largest changes.

	(A) Δ[N-NO3] in PRB Capsule		**(B) Δ[N-NO3] in soil core**		**(C) Δ[N-NO3] in total system**[a]	
Treatment	Mean (mg/L)	Median (mg/L)	Mean (mg/L)	Median (mg/L)	Mean (mg/L)	Median (mg/L)
NS	0.703	-0.150	0.112	-1.140	0.592	0.710
WC	-2.767	-1.255	-2.667	-2.155	-0.100	0.000
ALM50	**-7.068**	**-6.930**	**-4.653**	**-4.650**	**-2.274**	**-3.455**
ALM25	-4.754	-6.640	-4.243	-4.560	-1.120	-1.410
ALM10	-2.052	-1.30	-2.228	-2.205	-0.220	-0.170

[a] Total system is defined as $[N\text{-}NO3]_{EFF} - [N\text{-}NO3]_{INF}$

Table 13. Aggregation of data showing nitrate, nitrite and isotopes of nitrate ($\delta^{15}N$ and $\delta^{18}O$) for treatments: NS, WC, ALM50, and ALM10[a] (lab samples) and NS, WC, ALM (field samples).

Field or Lab	**Treatment**	Depth	[N-NO3] mg/L	[N-NO2] mg/L	$\delta^{15}N$ ‰	$\delta^{18}O$ ‰
lab	NS	0	8.60	0.01	0.35	49.64
lab	NS	PRB	7.38	0.29	5.39	50.64
lab	NS	100	4.30	0.01	2.84	50.44
lab	WC	0	12.57	0.00	0.30	50.71
lab	WC	PRB	3.11	0.02	10.12	47.21
lab	WC	100	4.68	0.05	12.16	44.05
lab	ALM50	0	10.98	0.00	0.36	49.62
lab	ALM50	PRB	5.41	2.03	4.48	54.45
lab	ALM50	100	0.63	3.89	9.16	57.77
lab	ALM10	0	6.85	0.00	0.42	51.83
lab	ALM10	PRB	4.25	0.06	2.63	53.18
lab	ALM10	100	3.62	0.09	4.58	53.31
field	NS	Inflow	0.61	0.01	7.98	7.76
field	NS	30 cm-bgs	0.62	0.01	7.80	7.60
field	NS	50 cm-bgs	0.64	0.00	7.43	5.98
field	WC	Inflow	1.36	0.02	8.23	7.07
field	WC	30 cm-bgs	1.58	0.02	6.87	6.25
field	WC	50 cm-bgs	0.58	0.04	15.00	10.87
field	ALM	Inflow	1.77	0.02	7.98	6.62
field	ALM	30 cm-bgs	1.63	0.02	7.67	6.44
field	ALM	50 cm-bgs	1.59	0.02	7.60	6.93

[a] ALM25 samples were not measured for isotopes of nitrate in the initial analysis. These samples will be analyzed in future work.

Bibliography

Babbitt, C., Gibson, K., Sellers, S., Brozovic, N., Saracino, A., Hayden, A., Hall, M., Zellmer, S. (2018). The Future of Groundwater in California: Lessons in Sustainable Management from Across the West. Daughtery Water for Food Global Institute: Faculty Publications. https://digitalcommons.unl.edu/wffdocs/86/

Beckman Coulter, 2011. Instruction for Use, LS 13 320 Laser Diffraction Particle Size Analyzer, PN B05577AB, 246 pp.

United States Department of Agriculture. (2023, July 12). 2023 California Almond Objective Measurement Report. https://www.nass.usda.gov/Statistics_by_State/California/Publications/Specialty_and_Other_Releases/Almond/Objective-Measurement/2023almondOM.pdf

Befus, K.M., Barnard, P.L., Hoover, D.J. Hart, J.A. Finzi, Voss, C.I. (2020). Increasing threat of coastal groundwater hazards from sea-level rise in California. Nat. Climate Change, 10, 946–952. https://doi.org/10.1038/s41558-020-0874-1

Beganskas, S., Gorski, G., Weathers, T., Fisher, A. T., Schmidt, C., Saltikov, C., Redford, K., Stoneburner, B., Harmon, R., & Weir, W. (2018). A horizontal permeable reactive barrier stimulates nitrate removal and shifts microbial ecology during rapid infiltration for managed recharge. Water Research, 144, 274-284. https://doi.org/10.1016/j.watres.2018.07.039

Beganskas, S., Young, K.S., Fisher, A.T. Harmon, R., Lozano, S. (2019). Runoff Modeling of a Coastal Basin to Assess Variations in Response to Shifting Climate and Land Use: Implications for Managed Recharge. Water Resource Management, 33, 1683–1698. https://doi.org/10.1007/s11269-019-2197-4

Bekele, E., Toze, S., Patterson, B., Higginson, S. (2011). Managed aquifer recharge of treated wastewater: Water quality changes resulting from infiltration through the vadose zone. Water Research, 45 (17), 5764-5772. https://doi.org/10.1016/j.watres.2011.08.058

Bouwer, H. (2002). Artificial Recharge of Groundwater: Hydrogeology and Engineering. Hydrogeology Journal, 10, 121-142. https://doi.org/10.1007/s10040-001-0182-4

Casciotti K. L. (2016). Nitrogen and Oxygen Isotopic Studies of the Marine Nitrogen Cycle. Annual review of marine science, 8, 379–407. https://doi.org/10.1146/annurev-marine-010213-135052

Davison, W., Woof, C., & Rigg, E. (1982). The dynamics of iron and manganese in a seasonally anoxic lake; direct measurement of fluxes using sediment traps.

Limnology and Oceanography, 27(6), 987-1003. https://doi.org/10.4319/lo.1982.27.6.0987

Garza-Díaz, L. E., DeVincentis, A. J., Sandoval-Solis, S., Azizpour, M., Ortiz-Partida, J. P., Mahlknecht, J., Cahn, M., Medellín-Azuara, J., ASCE, M., Zaccaria, D., Kisekka, I. (2019). Land-Use Optimization for Sustainable Agricultural Water Management in Pajaro Valley, California. Journal of Water Resources Planning and Management, 145(12). https://doi.org/10.1061/(ASCE)WR.1943-5452.0001117

Gilbert, O., Pomierny, S., Rowe, I., Kalin, R. M. (2008). Selection of organic substrates as potential reactive materials for use in a denitrification permeable reactive barrier (PRB). Bioresource Technology, 99(16), 7587-7596. https://doi.org/10.1016/j.biortech.2008.02.012

Gorski, G., Dailey, H., Fisher, A. T., Schrad, N., & Saltikov, C. (2020). Denitrification during infiltration for managed aquifer recharge: Infiltration rate controls and microbial response. Science of The Total Environment, 727, 138642. https://doi.org/10.1016/j.scitotenv.2020.138642

Gorski, G., Fisher, A. T., Beganskas, S., Weir, W. B., Redford, K., Schmidt, C., & Saltikov, C. (2019). Field and Laboratory Studies Linking Hydrologic, Geochemical, and Microbiological Processes and Enhanced Denitrification during Infiltration for Managed Recharge. Environmental science & technology, 53(16), 9491–9501. https://doi.org/10.1021/acs.est.9b01191

Granger, J., Sigman, D. M., Lehmann, M. F., & Tortell, P. D. (2008). Nitrogen and oxygen isotope fractionation during dissimilatory nitrate reduction by denitrifying bacteria. Limnology and Oceanography, 53(6), 2533-2545. https://doi.org/10.4319/lo.2008.53.6.2533

Grau-Martínez, A., Folch, A., Torrentó, C., Valhondo, C., Barba, C., Domènech, C., Soler, A., Otero, N. (2018). Monitoring induced denitrification during managed aquifer recharge in an infiltration pond. Journal of Hydrology, 561, 123-135. https://doi.org/10.1016/j.jhydrol.2018.03.044

Hanson, R. T. (2003). Geohydrologic Framework of Recharge and Seawater Intrusion in the Pajaro Valley, Santa Cruz and Monterey Counties, California. U.S. Geological Survey, Water Resources Investigations Report 03-4096. https://pubs.usgs.gov/wri/wri034096/

Knowles, R. (1982). Denitrification. Microbiological Reviews. 46(1), 43-70, https://doi.org/10.1128/mr.46.1.43-70.1982

Korom, S. F. (1992), Natural denitrification in the saturated zone: A review, Water Resources Research, 28(6), 1657–1668, https://doi.org/10.1029/92WR00252

Kumar, M., & Lin, J. G. (2010). Co-existence of anammox and denitrification for simultaneous nitrogen and carbon removal--Strategies and issues. Journal of hazardous materials, 178(1-3), 1–9. https://doi.org/10.1016/j.jhazmat.2010.01.077

Li, S., Diao, M., Liao, Y., & Ji, G. (2023). Performance, microbial growth and community interactions of iron-dependent denitrification in freshwaters. Environment International, 178, 108124. https://doi.org/10.1016/j.envint.2023.108124

Li, G. L., Zhou, C. H., Fiore, S., & Yu, W. H. (2019). Interactions between microorganisms and clay minerals: New insights and broader applications. Applied Clay Science, 177, 91-113. https://doi.org/10.1016/j.clay.2019.04.025

Masciopinto, C. (2013). Management of aquifer recharge in Lebanon by removing seawater intrusion from coastal aquifers. Journal of Environmental Management, 130, 306-312. https://doi.org/10.1016/j.jenvman.2013.08.021

McCasland, M., Trautmann, N. M., Porter, K.S., Wagenet, R.J. (1985). Nitrate: Health Effects in Drinking Water. Natural Resources. 400-402.
Shuval, H. I., Gruener, N., (2013). Infant Methemoglobinemia and other health effects of nitrates in drinking water. Proceedings of the Conference on Nitrogen As a Water Pollutant, 8.4, 183-193. https://doi.org/10.1016/B978-1-4832-1344-6.50017-4.

Mikutta, R., Kleber, M., Kaiser, K., & Jahn, R. (2005). Review. Soil Science Society of America Journal, 69(1), 120-135. https://doi.org/10.2136/sssaj2005.0120

Pensky, J., Fisher, A. T., Gorski, G., Schrad, N., Bautista, V., & Saltikov, C. (2023). Linking nitrate removal, carbon cycling, and mobilization of geogenic trace metals during infiltration for managed recharge. Water research, 239, 120045. https://doi.org/10.1016/j.watres.2023.120045

Robertson, W.D., Blowes, D.W., Ptacek, C. J., Cherry, J. A., Long-term performance of in situ reactive barriers for nitrate remediation. Groundwater, 38(5), 689-695. https://doi.org/10.1111/j.1745-6584.2000.tb02704.x

Schipper, L.A., Robertson, W.D., Gold, A. J., Jaynes, D. B., Cameron, S. C. (2010). Denitrifying bioreactors-An approach for reducing nitrate loads to receiving waters. Ecological Engineering, 36(11), 1532-1543, https://doi.org/10.1016/j.ecoleng.2010.04.008

Schmidt, C. M., Fisher, A. T., Racz, A. J., Lockwood, B. S., Huertos, M. L. (2011). Linking Denitrification and Infiltration Rates during Managed Groundwater Recharge. Environmental Science & Technology, 45(22), 9634-9640. https://doi.org/10.1021/es2023626

Smith, R. L., Böhlke, J. K., Song, B., Tobias, C. R. (2015). Role of Anaerobic Ammonium Oxidation (Anammox) in Nitrogen Removal from a Freshwater Aquifer. Environmental Science & Technology, 49(20), 12169-12177. https://doi.org/10.1021/acs.est.5b02488

Soares, M.I.M. (2000). Biological Denitrification of Groundwater. Water, Air, and Soil Pollution, 123, 183-193. https://doi.org/10.1023/A:1005242600186

Soil Survey Staff, U.S. Department of Agriculture, 2014. Soil Survey Geographic (SSURGO) Database. Available from: https://gdg.sc.egov.usda.gov/GDGOrder

Taylor, R., Scanlon, B., Döll, P. et al. (2013). Ground water and climate change. Nature Climate Change, 3, 322–329. https://doi.org/10.1038/nclimate1744

Ward, M. H., Cerhan, J. R., Colt, J. S., & Hartge, P. (2006). Risk of Non-Hodgkin Lymphoma and Nitrate and Nitrite from Drinking Water and Diet. Epidemiology, 17(4), 375–382. http://www.jstor.org/stable/20486238